
Article:
Shen, Q., Liu, W. orcid.org/0000-0003-2968-2888, Cui, W. et al. (2 more authors) (2019) Simplified and enhanced multiple level nested arrays exploiting high order difference co-arrays. IEEE Transactions on Signal Processing, 67 (13). pp. 3502-3515. ISSN 1053-587X

https://doi.org/10.1109/tsp.2019.2914887

Simplified and Enhanced Multiple Level Nested Arrays Exploiting High Order Difference Co-Arrays

Qing Shen, Wei Liu, *Senior Member, IEEE,* Wei Cui, Siliang Wu, and Piya Pal, *Member, IEEE*

***Abstract*—Based on the high order difference co-array concept, an enhanced four level nested array (E-FL-NA) is first proposed, which optimizes the consecutive lags at the fourth order difference co-array stage. To simplify sensor location formulations for comprehensive illustration and also convenient structure construction, a simplified and enhanced four level nested array (SE-FL-NA) is then proposed, whose performance is compromised but still better than the four level nested array (FL-NA). This simplified structure is further extended to the higher order case with multiple sub-arrays, referred to as simplified and enhanced multiple level nested arrays (SE-ML-NAs), where significantly increased degrees of freedom (DOFs) can be provided and exploited for underdetermined DOA estimation. Simulation results are provided to demonstrate the performance of the proposed E-FL-NA, while a higher number of detectable sources is achieved by the SE-ML-NA with a limited number of physical sensors.**

***Index Terms*—sparse array, higher order, difference co-array, direction of arrival estimation, nested array.**

I. Introduction

Direction of arrival (DOA) estimation is a fundamental problem in array signal processing [1]–[4], and has been studied extensively over the decades. It is well known that for an N-sensor uniform linear array (ULA), only $N-1$ degrees of freedom (DOFs) can be exploited for DOA estimation by commonly used subspace based methods such as MUSIC [5], ESPRIT [6], and compressive sensing (CS) based methods such as ℓ_1-SVD [7].

In the past few years, DOA estimation for the underdetermined case where the number of sources is larger than the number of physical sensors has attracted significant attention [8], and various sparse arrays [9]–[11] have been proposed as possible solutions, among which nested arrays [12] and co-prime arrays [13], [14] are the most notable configurations presented recently. In [15], co-prime arrays with compressed inter-element spacing (CACIS) and co-prime arrays with displaced subarrays (CADiS) are proposed, while super nested arrays [16], [17] and augmented nested arrays [18] are introduced to reduce mutual coupling. Furthermore, thinned co-prime arrays are proposed in [19], [20], offering further increased DOFs for DOA estimation. Moreover, a single ULA acting as two sub-arrays of a co-prime array configuration at two continuous-wave signals of co-prime frequencies is employed in [21]. This idea is extended to multiple frequencies in [22]–[24]. Based on the co-array equivalence, except for the spatial smoothing based subspace approaches such as MUSIC (SS-MUSIC) [12]–[14], [25], [26], DOA estimation algorithms under the CS framework [15], [27]–[29] can also be utilized.

Most of the aforementioned works are based on the second order difference co-arrays, and their Cramér-Rao Bounds (CRBs) are given in [30]–[32]. On the other hand, high order statistics have been exploited for underdetermined DOA estimation over the decades. The fourth order cumulants based DOA estimation methods are proposed in [33], [34], and its virtual array concept is presented in [35]. Recently, the $2q$-th order cumulants are exploited for DOA estimation and its performance such as DOFs and resolution power improves with the increase of q [36]–[38]. Then, the $2q$-th order difference co-array concept is proposed in [39], corresponding to the manifold of the virtual array configuration generated by vectorizing the $2q$-th order circular cumulant matrix. Furthermore, multiple level nested arrays (ML-NAs) are introduced with a substantial increase in the number of DOFs [39]. SS-MUSIC is applied to find the DOAs for the narrowband case [39], while the group sparsity based method [28], [40] and a focusing-based method within the CS framework is presented in [41] for the wideband case.

Although the ML-NA provides a systematic way for convenient structure construction, it is not optimum and further improvement is possible. Our first attempt in [42], [43] gives a sparse array construction method with the fourth order difference co-array enhancement by introducing a third sub-array to the nested array and co-prime array, respectively, forming the structures referred to as SAFOE-NA and SAFOE-CPA, and a DOA estimation method for nonstationary sources based on the fourth order difference co-arrays is presented in [43]. An expanding and shift scheme is proposed in [44], leading to structures with more DOFs at the fourth order difference co-array stage, i.e., EAS-NA-NA and EAS-NA-CPA. In [45], a two level nested array for fourth order cumulant based DOA estimation (2L-FO-NA) is proposed with hole-free co-arrays achieved, and more potential DOFs can be provided compared with the SAFOE-NA [42] when the sensor number is smaller than 12. Based on the fourth order difference co-arrays, an extension of co-prime arrays is presented in [46], and DOA estimation for non-circular signals is studied in [47].

In this paper, we further investigate the array structure optimization problem exploiting the fourth order difference co-array concept. Based on the property of permutation invari-

This work was supported in part by the National Natural Science Foundation of China under Grants 61801028 and 61628101, and the China Postdoctoral Science Foundation under Grant 2018M631357. Piya Pal is supported by NSF CAREER Award ECCS 1700506 and ONR Award N00014-18-1-2038. Corresponding authors: W. Liu and W. Cui.

Q. Shen, W. Cui and S. Wu are with the School of Information and Electronics, Beijing Institute of Technology, Beijing, 100081, China (e-mail: qing-shen@outlook.com, cuiwei@bit.edu.cn, siliangw@bit.edu.cn); Q. Shen is also with the Department of Electronic and Electrical Engineering, University of Sheffield, Sheffield, S1 3JD, UK.

W. Liu is with the Department of Electronic and Electrical Engineering, University of Sheffield, Sheffield, S1 3JD, UK (e-mail: w.liu@sheffield.ac.uk).

P. Pal is with the Department of Electrical and Computer Engineering, University of California, San Diego, USA (e-mail: pipal@eng.ucsd.edu).

ance, the fourth order difference co-array can be considered as a further second order difference co-array, which is based on the virtual array corresponding to the first-level second order difference co-array of the original physical array. Then, an array construction method is proposed by constructing two sub-arrays simultaneously to form an enhanced four level nested array (E-FL-NA), maximizing the consecutive co-array lags by arranging the virtual ULA sets associated with extra sensors to be adjacent to each other. By exploiting the physical array aperture along with the virtual array aperture and its symmetric information, a great increase in the number of consecutive co-array lags is achieved.

The formulations of sensor positions in the constructed E-FL-NA and other configurations such as SAFOE-NA and EAS-NA-NA are complicated, and will be much more complicated and difficult to follow when extended to the $2q$-th order case following a similar construction method, where the sub-array sensor position will be a linear combination of the virtual ULA apertures at the lower order difference co-array stage, and each aperture is also a linear combination of the ULA apertures at the lower order difference co-array stage.

Therefore, we simplify the sensor distribution formulations for convenient structure construction and comprehensive illustration with an assistant sensor at the zeroth position, which is finally removed from our resultant simplified and enhanced four level nested array (SE-FL-NA). Except for the ML-NA [39], constructing sparse array structures for higher order difference co-arrays is still an unsolved problem. By investigating the $2q$-th order difference co-arrays, it can be considered as the difference between the second order difference co-array and the $2(q-1)$-th order difference co-array, and there would be potential increase of DOFs at each $2m$-th ($1 \leq m \leq q$) order difference co-array stage. Then, the simplified and enhanced configuration SE-FL-NA is extended to the $2q$-th order based on the link between the $2q$-th order and the $2(q-1)$-th order difference co-arrays, forming a generalized and optimized configuration, referred to as simplified and enhanced $2q$-th level nested array (SE-$2q$L-NA), providing a convenient construction for the exploration of high order difference co-arrays. It is noted that the formulations of the sensor positions in the SE-ML-NA are independent of the virtual ULA apertures or any other information at the lower order stage. As a result, the SE-ML-NA is far more comprehensive.

Our contributions are therefore: 1) introducing the fourth order difference co-array concept from the perspective of applying the second order difference co-array twice, and developing an enhanced four level nested array to maximize the consecutive co-array lags, achieving a higher number of DOFs than existing configurations; 2) for convenient structure construction, sensor position formulations are further simplified; 3) the sparse array construction method is extended to high order difference co-arrays, and a simplified and enhanced multiple level nested array (SE-ML-NA) is proposed with simple formulations for each sensor location.

This paper is organized as follows. Definition of the high order difference co-array and the ML-NA are introduced in Section II. The proposed enhanced four level nested arrays exploring the fourth order difference co-arrays is presented in Section III, while the sparse array design method for the high order co-array case and the simplified and enhanced multiple nested arrays are proposed in Section IV with the exact number of consecutive lags derived. Simulation results are provided in Section V, and conclusions are drawn in Section VI.

II. High-Order Difference Co-Array Perspective and Multiple Level Nested Arrays

A. Virtual Array Generation from the High Order Difference Co-Array Perspective

Consider a general linear array with N physical sensors. The set of sensor positions $\mathbb{S}$ is expressed as

$$\mathbb{S} = \left\{ \hbar_0 \cdot d, \hbar_1 \cdot d, \ldots, \hbar_{N-1} \cdot d \right\} , \tag{1}$$

where $\hbar_n \cdot d$ is the position of the n-th sensor, $n = 0, 1, \ldots, N-1$, and d is the unit spacing satisfying $d \leq \lambda/2$ with λ being the signal wavelength.

Definition 1: For the linear array in (1), the set of the $2q$-th (q is an integer and $q \geq 1$) order difference co-array is defined as [39]

$$\mathbb{C}_{2q} = \Phi_{2q} \cdot d , \tag{2}$$

where the set of the $2q$-th order difference co-array lags

$$\Phi_{2q} = \left\{ \sum_{m=1}^{q} \hbar_{n_m} - \sum_{m=q+1}^{2q} \hbar_{n_m} \mid 0 \leq n_m \leq N-1 \right\} . \tag{3}$$

To exploit the increased DOFs offered by the $2q$-th order difference co-array for underdetermined DOA estimation, a virtual array signal model with a series of virtual sensors distributed at the set $\mathbb{C}_{2q}$ is required. Assume that there are K mutually uncorrelated zero-mean narrowband signals $s_k(t)$ impinging from the far-field directions $\theta_k, k = 1, 2, \ldots, K$, respectively. The array output model in discrete version is

$$\mathbf{x}[i] = \mathbf{A}(\boldsymbol{\theta})\mathbf{s}[i] + \bar{\mathbf{n}}[i] , \tag{4}$$

where $\mathbf{x}[i]$ is the observed $N \times 1$ signal vector, $\mathbf{s}[i] = [s_1[i], \ldots, s_K[i]]^T$ is the source signal vector consisting of all the impinging signals, and $\{\cdot\}^T$ denotes the transpose operation. $\bar{\mathbf{n}}[i]$ represents the noise vector, and the $N \times K$ steering matrix $\mathbf{A}(\boldsymbol{\theta}) = [\mathbf{a}(\theta_1), \ldots, \mathbf{a}(\theta_K)]$, with its k-th column vector $\mathbf{a}(\theta_k)$ being the steering vector corresponding to the k-th source signal, expressed as

$$\mathbf{a}(\theta_k) = \left[e^{-j\frac{2\pi\hbar_0 d}{\lambda}\sin(\theta_k)}, \ldots, e^{-j\frac{2\pi\hbar_{N-1} d}{\lambda}\sin(\theta_k)} \right]^T . \tag{5}$$

By calculating the $2q$-th order circular cumulants, a cumulant matrix $\mathbf{C}_{2q,\mathbf{x}}(\mu)$ for the arrangement indexed by μ ($0 \leq \mu \leq q$) can be obtained, given by [36], [37], [39]

$$\begin{aligned} \mathbf{C}_{2q,\mathbf{x}}(\mu) = &\sum_{k=1}^{K} c_{2q,s_k} \left[\mathbf{a}(\theta_k)^{\otimes\mu} \otimes \mathbf{a}(\theta_k)^{*\otimes(q-\mu)} \right] \\ &\times \left[\mathbf{a}(\theta_k)^{\otimes\mu} \otimes \mathbf{a}(\theta_k)^{*\otimes(q-\mu)} \right]^H + \sigma_{\bar{n}}^2 \mathbf{I}_{N^q} \cdot \delta(q-1) , \end{aligned} \tag{6}$$

where $\{\cdot\}^*$ is the conjugate operation and $\{\cdot\}^H$ represents the Hermitian transpose. $\mathbf{a}(\theta_k)^{\otimes\mu} \triangleq \mathbf{a}(\theta_k) \otimes \mathbf{a}(\theta_k) \otimes \ldots \otimes \mathbf{a}(\theta_k)$ is an $N^\mu \times 1$ column vector, with the Kronecker product ($\otimes$) of in total μ of the vectors $\mathbf{a}(l, \theta_k)$. $\sigma_{\bar{n}}^2$ is the noise power,

$\mathbf{I}_{N^q}$ is the $N^q \times N^q$ identity matrix, and $\delta(\cdot)$ is the Kronecker delta function. c_{2q,s_k} is the $2q$-th order circular auto-cumulant of $s_k[i]$, obtained by [48]

$$c_{2q,s_k} = \mathrm{Cum}\left\{ \underbrace{s_k[i],\ldots,s_k[i]}_{q \text{ times}}, \overbrace{s_k^*[i],\ldots,s_k^*[i]}^{q \text{ times}} \right\} , \quad (7)$$

with $\mathrm{Cum}\{\cdot\}$ denoting the cumulant operator. For zero-mean white Gaussian noise, its $2q$-th ($q \geq 2$) order auto-cumulant is zero. Therefore, the second term in (6) related to noise is zero for $q \geq 2$.

According to Theorem 1 in [39], vectorizing the $2q$-th cumulant matrix $\mathbf{C}_{2q,\mathbf{x}}(\mu)$ yields a virtual array model independent of μ

$$\mathbf{z} = \mathrm{vec}\left\{\mathbf{C}_{2q,\mathbf{x}}(\mu)\right\} = \mathbf{B}(\boldsymbol{\theta})\mathbf{u} + \sigma_{\tilde{n}}^2 \widetilde{\mathbf{I}}_{N^{2q}} \cdot \delta(q-1) , \quad (8)$$

where $\widetilde{\mathbf{I}}_{N^{2q}}$ is an $N^{2q} \times 1$ column vector obtained by vectorizing the identity matrix $\mathbf{I}_{N^q}$. $\mathbf{u} = [c_{2q,s_1},\ldots,c_{2q,s_K}]$ is the equivalent signal vector consisting of all the $2q$-th order auto-cumulants of the source signals, while $\mathbf{B}(\boldsymbol{\theta}) = [\mathbf{b}(\theta_1),\ldots,\mathbf{b}(\theta_K)]$ is the equivalent steering matrix behaving like the manifold of virtual sensors located at the set of the $2q$-th order difference co-array $\mathbb{C}_{2q}$ in (2), with each of its column vectors expressed as

$$\begin{aligned}\mathbf{b}(\theta_k) = &\left[\mathbf{a}(\theta_k)^{\otimes\mu} \otimes \mathbf{a}(\theta_k)^{*\otimes(q-\mu)}\right]^* \\ &\otimes \left[\mathbf{a}(\theta_k)^{\otimes\mu} \otimes \mathbf{a}(\theta_k)^{*\otimes(q-\mu)}\right] .\end{aligned} \quad (9)$$

B. Nested Arrays with Multiple Levels

The number of virtual sensors in $\mathbb{C}_{2q}$ is much larger than the number of physical sensors, and $2q$-level nested arrays ($2q$L-NAs) [39] are designed to optimize the virtual ULA segment included in the $2q$-th order difference co-array. These increased DOFs offered by the virtual ULA can be exploited by a spatial smoothing based subspace method [12], [39].

Definition 2: A typical $2q$-level nested array [39] consists of $2q$ uniform linear sub-arrays. Denote $N_0 = 1$, for $1 \leq m \leq 2q-1$, the m-th sub-array has $N_m - 1$ sensors located at

$$\mathbb{S}_m = \left\{ nd\left(\prod_{\tilde{m}=0}^{m-1} N_{\tilde{m}}\right) \mid n = 1,2,\ldots,N_m - 1 \right\} , \quad (10)$$

while the sensors of the $2q$-th sub-array with N_{2q} sensors are located at

$$\mathbb{S}_{2q} = \left\{ nd\left(\prod_{\tilde{m}=0}^{2q-1} N_{\tilde{m}}\right) \mid n = 1,2,\ldots,N_{2q} \right\} . \quad (11)$$

Then, there are $N = \sum_{m=1}^{2q}(N_m - 1) + 1$ physical sensors in total.

By Lemma 1 in [39], the number of virtual ULA sensors in the $2q$-th order difference co-array of the $2q$L-NA reaches

$$M_{\mathrm{ML}} = 2(\prod_{m=1}^{2q} N_m + \prod_{m=1}^{2q-1} N_m) - 1 . \quad (12)$$

The maximum number of virtual ULA sensors included in the $2q$-th order difference co-array $\mathbb{C}_{2q}$ indicates the maximum number of consecutive lags in Φ_{2q}, and with an appropriate unit spacing $d \leq \lambda/2$ between adjacent virtual sensors to avoid spatial aliasing, DOFs provided by this ULA segment can be exploited through various DOA estimation methods based on (8). In particular, spatial smoothing based subspace methods in [12]–[14], [39] and the subspace method based on a reshaping process to form a Toeplitz matrix in [49] can only exploit the DOFs provided by the virtual ULA segment, while the CS-based method [15], [27], [28] is capable of exploiting the DOFs provided by all the unique virtual sensors.

Remark 1: The number of virtual sensors of the $2q$-th order difference co-array is N^{2q} including redundancies. The $2q$L-NA gives rise to $O(N^{2q})$ consecutive lags at the $2q$-th order stage compared with N^{2q} total lags including redundancies, showing that it is an effective and attractive structure, although it is not optimum and further improvement is possible. As will be demonstrated, in our proposed array construction methods, the consecutive segments in Φ_{2q} associated with introduced sensors are designed to be adjacent to each other. In this way, based on a standard TL-NA with certain redundancies at the $2q$-order difference co-array stage, we optimize the redundancies introduced by each additional sensor under construction, and therefore both the consecutive lags and the unique lags are increased compared with the $2q$L-NA. As in [15], [39], [42], [43], the achievable number of consecutive virtual sensors is considered for quantitative evaluation, comparison, and optimal design.

III. Sparse Array Optimization Based on the Fourth Order Difference Co-Array Concept

For the TL-NAs, their second order difference co-arrays provide a significant increase in DOFs by exploring the features of the given physical geometry. However, the non-uniform feature of the generated virtual array at the second order is not optimized for the fourth order difference co-array usage, and the increase of DOFs is limited at the latter stage. By analysing the consecutive lags associated with the introduced additional sensors, we optimize/adjust the non-uniformity of the second-order difference co-array so that the consecutive segments associated with introduced sensors at the fourth-order difference co-array stage are adjacent to each other, leading to an even higher number of DOFs.

A. Fourth Order Difference Co-Array Perspective

According to *Definition 1*, the second order difference co-array (also known as difference co-array) is defined as

$$\begin{aligned}&\mathbb{C}_{\mathbf{2}} = \Phi_2 \cdot d , \\ &\Phi_2 = \{\hbar_{n_1} - \hbar_{n_2} \mid n_1, n_2 = 0,1,\ldots,N-1\} .\end{aligned} \quad (13)$$

Similarly, the fourth order difference co-array is expressed as $\mathbb{C}_{\mathbf{4}} = \Phi_4 \cdot d$, where for $n_1, n_2, n_3, n_4 = 0,1,\ldots,N-1$, the set of the fourth order difference co-array lags

$$\begin{aligned}\Phi_4 &= \{\hbar_{n_1} + \hbar_{n_2} - \hbar_{n_3} - \hbar_{n_4}\} \\ &= \{(\hbar_{n_1} - \hbar_{n_3}) - (\hbar_{n_4} - \hbar_{n_2})\} \\ &= \{\mu_1 - \mu_2 \mid \mu_1, \mu_2 \in \Phi_2\} ,\end{aligned} \quad (14)$$

where $\mu_1 = \hbar_{n_1} - \hbar_{n_3} \in \Phi_2$ and $\mu_2 = \hbar_{n_4} - \hbar_{n_2} \in \Phi_2$.

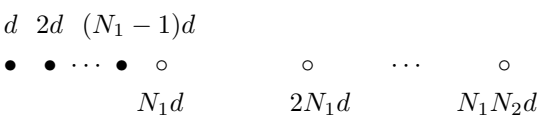

Fig. 1. Structure of a general TL-NA with two uniform linear sub-arrays.

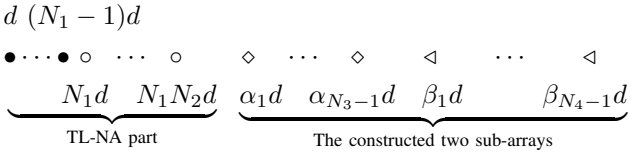

Fig. 2. A general structure of the E-FL-NA, consisting of four uniform linear sub-arrays, with their sensors indicated as •, ○, ◇, and ◁, respectively.

From this point of view, the fourth order difference co-array can be obtained by calculating the second order difference co-array of the virtual array generated at the second order difference co-array stage with virtual sensors given in $\mathbb{C}_2$.

A general TL-NA according to *Definition 2* for $q = 1$ is shown in Fig. 1, where the first sub-array has $N_1 - 1$ sensors starting from the position $1d$ with an inter-element spacing d, and the second sub-array has N_2 sensors starting from the position $N_1 d$ with the inter-element spacing $N_1 d$. Denote $\mathbb{S}_m$ as the sensor position set of the m-th sub-array, the sensor positions of a TL-NA can be expressed as

$$\begin{aligned} \mathbb{S}_1 &= \{n_1 d \mid n_1 = 1, 2 \ldots, N_1 - 1\} \ , \\ \mathbb{S}_2 &= \{n_2 N_1 d \mid n_2 = 1, 2 \ldots, N_2\} \ . \end{aligned} \tag{15}$$

There are $N_1 + N_2 - 1$ physical sensors in total, and the second order difference co-array lags achieved can be expressed as

$$\Phi_2 = \{\mu \mid -N_1 N_2 + 1 \leq \mu \leq N_1 N_2 - 1, \mu \in \mathbb{Z}\} \ , \tag{16}$$

where $\mathbb{Z}$ denotes the set of all integers.

Note that Φ_2 of the TL-NA only contains consecutive integers from $-N_1 N_2 + 1$ to $N_1 N_2 - 1$, corresponding to a ULA with $2N_1 N_2 - 1$ virtual sensors at the second-order difference co-array stage. Furthermore, the four level nested array (FL-NA) is not optimum since the physical array aperture and the symmetric features in the second order difference co-array have not been fully exploited in array construction.

B. Extended Four Level Nested Arrays with Fourth Order Difference Co-Array Enhancement

As illustrated in our earlier work [42], the sparse array with the fourth order difference co-array enhancement based on a TL-NA (SAFOE-NA) provides a larger number of consecutive lags than the existing FL-NA when the sensor number $N \leq 20$. To form a better configuration compared with both the SAFOE-NA and the FL-NA with a consistently larger number of consecutive lags for different N, an enhanced four level nested array is proposed by constructing two extra sub-arrays based on the TL-NA simultaneously.

Proposition 1: The enhanced four level nested array (E-FL-NA) consisting of four uniform linear sub-arrays is shown in Fig. 2, where for $d_{N_4} = N_3(2N_1N_2 - 1) + N_1N_2 - 1$, the locations of the E-FL-NA are given as

$$\begin{aligned} \mathbb{S}_1 &= \{n_1 d \mid n_1 = 1, 2 \ldots, N_1 - 1\} \ , \\ \mathbb{S}_2 &= \{n_2 N_1 d \mid n_2 = 1, 2 \ldots, N_2\} \ . \\ \mathbb{S}_3 &= \{(3N_1N_2 - 1)d + (n_3 - 1)(2N_1N_2 - 1)d \mid \\ &\qquad n_3 = 1, 2, \ldots, N_3 - 1\} \ , \\ \mathbb{S}_4 &= \{2N_3(2N_1N_2 - 1)d + (n_4 - 1)d_{N_4} d \mid \\ &\qquad n_4 = 1, 2, \ldots, N_4 - 1\} \ . \end{aligned} \tag{17}$$

The set of the consecutive fourth order difference co-array lags Φ_{C}^4 of our proposed structure is updated to

$$\Phi_{\mathrm{C}}^4 = \left\{\mu \mid -M_{\max}^4 \leq \mu \leq M_{\max}^4, \mu \in \mathbb{Z}\right\} \ , \tag{18}$$

where $M_{\max}^4 = N_3N_4(2N_1N_2 - 1) + (N_4 - 1)(N_1N_2 - 1) - 1$, and the number of consecutive lags is $2M_{\max}^4 + 1$.

Proof: Denote $\alpha_{n_3} d$ ($n_3 = 1, 2, \ldots, N_3 - 1$) and $\beta_{n_4} d$ ($n_4 = 1, 2, \ldots, N_4 - 1$) as the n_3-th sensor position of the third sub-array and the n_4-th sensor position of the fourth sub-array, respectively. Due to symmetry of the high order difference co-arrays, we only analyze the positive part.

By analyzing the cross-difference co-array between the introduced sensors and the original TL-NA sensors according to (16) with the consecutive integers ranging from $-N_1N_2 + 1$ to $N_1N_2 - 1$ in the original TL-NA, the sets of consecutive integers at the fourth order difference co-array stage associated with $\alpha_{n_3} d$ and $\beta_{n_4} d$ are given as

$$\begin{aligned} \phi_{\alpha_{n_3}} &= \left\{\mu \mid \nu_{\alpha_{n_3}} \leq \mu \leq \zeta_{\alpha_{n_3}}, \mu \in \mathbb{Z}\right\} \ , \\ \phi_{\beta_{n_4}} &= \left\{\mu \mid \nu_{\beta_{n_4}} \leq \mu \leq \zeta_{\beta_{n_4}}, \mu \in \mathbb{Z}\right\} \ , \end{aligned} \tag{19}$$

where

$$\begin{aligned} \nu_{\alpha_{n_3}} &= \alpha_{n_3} - 2N_1N_2 + 1, \ \zeta_{\alpha_{n_3}} = \alpha_{n_3} + N_1N_2 - 2 \ , \\ \nu_{\beta_{n_4}} &= \beta_{n_4} - 2N_1N_2 + 1, \ \zeta_{\beta_{n_4}} = \beta_{n_4} + N_1N_2 - 2 \ . \end{aligned} \tag{20}$$

Without loss of generality, assume that the fourth sub-array has the largest inter-element spacing, and $\beta_{n_4} > \alpha_{n_3}$, $\forall n_3 = 1, 2, \ldots, N_3 - 1$, $n_4 = 1, 2, \ldots, N_4 - 1$. By examining the fourth order cross-difference co-arrays between the third sub-array and the fourth sub-array, the set of consecutive lags associated with $\beta_{n_4} d - \alpha_{n_3} d$ according to (16) is given by

$$\varphi_{\alpha_{n_3}, \beta_{n_4}} = \left\{\mu \mid \nu_{\alpha_{n_3}, \beta_{n_4}} \leq \mu \leq \zeta_{\alpha_{n_3}, \beta_{n_4}}, \mu \in \mathbb{Z}\right\} \ , \tag{21}$$

with the lower bound and upper bound expressed as

$$\begin{aligned} \nu_{\alpha_{n_3}, \beta_{n_4}} &= \beta_{n_4} - \alpha_{n_3} - N_1N_2 + 1 \ , \\ \zeta_{\alpha_{n_3}, \beta_{n_4}} &= \beta_{n_4} - \alpha_{n_3} + N_1N_2 - 1 \ . \end{aligned} \tag{22}$$

To maximize the consecutive range associated with each sensor in the fourth sub-array, the following relationship should be satisfied to ensure the covered ranges with a fixed n_4 are adjacent to each other:

$$\zeta_{\alpha_{n_3+1}, \beta_{n_4}} + 1 = \nu_{\alpha_{n_3}, \beta_{n_4}} \ . \tag{23}$$

Then we can obtain the inter-element spacing of the third sub-array by solving (23), given by

$$d_{N_3} = \alpha_{n_3+1} - \alpha_{n_3} = 2N_1N_2 - 1 \ . \tag{24}$$

As a result, $\forall 1 \leq n_3 \leq N_3-1$, the set of consecutive integers associated with $\beta_{n_4}d$ is combined into

$$\begin{aligned}\varphi_{\alpha,\beta_{n_4}} &= \varphi_{\alpha_1,\beta_{n_4}} \bigcup \varphi_{\alpha_2,\beta_{n_4}} \cdots \bigcup \varphi_{\alpha_{N_3-1},\beta_{n_4}} \\ &= \left\{\mu \mid \nu_{\alpha_{N_3-1},\beta_{n_4}} \leq \mu \leq \zeta_{\alpha_1,\beta_{n_4}}, \mu \in \mathbb{Z}\right\} \ ,\end{aligned} \tag{25}$$

where

$$\begin{aligned}\nu_{\alpha_{N_3-1},\beta_{n_4}} &= \beta_{n_4} - \alpha_{N_3-1} - N_1N_2 + 1 \ , \\ \zeta_{\alpha_1,\beta_{n_4}} &= \beta_{n_4} - \alpha_1 + N_1N_2 - 1 \ .\end{aligned} \tag{26}$$

A straightforward idea is to arrange these sets $\varphi_{\alpha,\beta_{n_4}}$ to be adjacent to each other by ensuring $\nu_{\alpha_{N_3-1},\beta_{n_4}+1} = \zeta_{\alpha_1,\beta_{n_4}}+1$.

However, a further improvement can be achieved by ensuring $\phi_{\beta_{n_4}}$ in (19) and $\varphi_{\alpha,\beta_{n_4}}$ in (25) to be adjacent to form a larger set containing increased number of consecutive integers associated with $\beta_{n_4}d$, with the relationship expressed as

$$\begin{aligned}\nu_{\beta_{n_4}} &= \zeta_{\alpha_1,\beta_{n_4}} + 1 = \beta_{n_4} - 2N_1N_2 + 1 \\ &= \beta_{n_4} - \alpha_1 + N_1N_2 - 1 + 1 \ .\end{aligned} \tag{27}$$

Then, the starting position in the third sub-array is

$$\alpha_1 = 3N_1N_2 - 1 \ . \tag{28}$$

Therefore, a large set $\varphi_{\beta_{n_4}}$ of consecutive difference co-array lags associated with $\beta_{n_4}d$ is generated by

$$\begin{aligned}\psi_{\beta_{n_4}} &= \phi_{\beta_{n_4}} \bigcup \varphi_{\alpha,\beta_{n_4}} \\ &= \left\{\mu \mid \nu_{\alpha_{N_3-1},\beta_{n_4}} \leq \mu \leq \zeta_{\beta_{n_4}}, \mu \in \mathbb{Z}\right\} \ .\end{aligned} \tag{29}$$

By allowing $\nu_{\alpha_{N_3-1},\beta_{n_4+1}} = \zeta_{\beta_{n_4}} + 1$, the inter-element spacing of the fourth sub-array is

$$d_{N_4} = \beta_{n_4+1} - \beta_{n_4} = N_3(2N_1N_2 - 1) + N_1N_2 - 1 \ . \tag{30}$$

For $\beta_1 d$ in the fourth sub-array, the lower bound $\nu_{\alpha_{N_3-1},\beta_1}$ is arranged to be $\zeta_{\alpha_{N_3-1}}$ in (19) plus 1 for the fourth order difference co-array optimization, given by

$$\begin{aligned}\nu_{\alpha_{N_3-1},\beta_1} &= \zeta_{\alpha_{N_3-1}} + 1 = \alpha_{N_3-1} + N_1N_2 - 2 + 1 \\ &= \beta_1 - \alpha_{N_3-1} - N_1N_2 + 1 \ .\end{aligned} \tag{31}$$

Then we can obtain the starting sensor position as

$$\beta_1 = 2N_3(2N_1N_2 - 1) = \alpha_{N_3-1} + \beta_{n_4+1} - \beta_{n_4} \ . \tag{32}$$

Finally, β_{N_4-1} is expressed as

$$\begin{aligned}\beta_{N_4-1} &= \beta_1 + (N_4 - 1)\left(\beta_{n_4+1} - \beta_{n_4}\right) \\ &= N_3N_4(2N_1N_2 - 1) + (N_4 - 2)(N_1N_2 - 1) \ ,\end{aligned}$$

and the maximum integer in the set of consecutive fourth order difference co-array lags can be obtained as

$$\begin{aligned}M^4_{\max} &= \zeta_{\beta_{N_4-1}} = \beta_{N_4-1} + N_1N_2 - 2 \\ &= N_3N_4(2N_1N_2 - 1) + (N_4 - 1)(N_1N_2 - 1) - 1 \ .\end{aligned} \tag{33}$$

Remark 2-(1): $(N_1N_2-1)d$ is the original physical aperture of the TL-NA part, while $(2N_1N_2 - 1)d$ is the number of consecutive lags (virtual array aperture) at the second order difference co-array stage. The larger spacings in the extra two sub-arrays are due to exploration of the physical aperture and the symmetric information at the second order difference co-array stage, which is not exploited in the design of the FL-NA [39].

Remark 2-(2): Since $\alpha_1 - N_1N_2 = \alpha_{n_3+1} - \alpha_{n_3} = 2N_1N_2 - 1$ and $\beta_1 = \alpha_{N_3-1} + \beta_{n_4+1} - \beta_{n_4}$ as shown in (32), the last sensor in the original TL-NA can also be considered as part of the third sub-array located at $\alpha_0 d$, whereas $\alpha_{N_3-1}d$ can be treated as $\beta_0 d$ in the fourth sub-array. Therefore, the structure of our proposed E-FL-NA is similar to the FL-NA with its sensor number being $N = \sum_{m=1}^{4}(N_m - 1) + 1$.

Remark 2-(3): The number of consecutive lags $2M^4_{\max}+1$ is the aperture of the virtual ULA at the fourth order difference co-array stage, and according to (33), it contains the physical array aperture and the virtual ULA aperture at the second order stage. Furthermore, denote P_{2q} as the aperture of the (virtual) ULA at the $2q$-th order stage with $q = 0$ representing the physical array, the inter-element spacings of the latter two sub-arrays in (24) and (30) are a linear combination of the P_0 and P_2. When further extended to the high order case with a similar construction method, there is no doubt that the spacings of the $(2q-1)$-th and $2q$-th sub-arrays will be a linear combination of the apertures P_{2q_1} $(q_1 = 0, 1, \ldots, q-1)$, where each P_{2q_1} is also a linear combination of P_{2q_2} with $q_2 = 0, 1, \ldots, q_1 - 1$, leading to a much more complicated expressions for sensor positions which is extremely difficult to follow.

IV. Simplified and Enhanced Multiple Level Nested Arrays

As discussed in *Remark 2-(3)*, for a more comprehensive illustration and also convenient structure construction, we first modify the E-FL-NA into a simplified and enhanced four level nested array (SE-FL-NA) configuration by sacrificing some potential DOFs but leading to a much more simple formulations for sensor positions, and then extend it to the high order case with a simplified and enhanced multiple nested array (SE-ML-NA) proposed. It is noted that the sensor position formulations of the SE-ML-NA are independent of the apertures at the lower order difference co-array stage, and the number of DOFs provided by the SE-ML-NA is still much more than that of the ML-NA.

A. Simplified and Enhanced Four Level Nested Arrays

Proposition 2: The SE-FL-NA consists of four uniform linear sub-arrays, as shown in Fig. 3. The sets of sensor positions in each sub-array $\mathbb{S}_m$, $m = 1, 2, 3, 4$, can be expressed as

$$\begin{aligned}\mathbb{S}_1 &= \{n_1 d \mid n_1 = 1, 2, \ldots, N_1 - 1\} \ , \\ \mathbb{S}_2 &= \{n_2 N_1 d \mid n_2 = 1, 2, \ldots, N_2\} \ , \\ \mathbb{S}_3 &= \{n_3 2N_1N_2 d \mid n_3 = 1, 2, \ldots, N_3 - 1\} \ , \\ \mathbb{S}_4 &= \{n_4 2N_1N_2N_3 d \mid n_4 = 1, 2, \ldots, N_4\} \ .\end{aligned} \tag{34}$$

With $\sum_{m=1}^{4}(N_m-1)+2$ sensors in total, the set of consecutive lags at the fourth order difference co-array stage is

$$\Phi^4_{\max} = \left\{\mu \mid -M^4_{\max} \leq \mu \leq M^4_{\max}\right\} \ , \tag{35}$$

where $M^4_{\max} = 2N_1N_2N_3N_4 + N_1N_2$, and the number of consecutive co-array lags is $2M^4_{\max} + 1$.

Proof: To simplify the formulations of array apertures, a sensor at the zeroth position is added first. Denote $\alpha_{n_3}d$ $(n_3 = 1, 2, \ldots, N_3 - 1)$ and $\beta_{n_4}d$ $(n_4 = 1, 2, \ldots, N_4)$ as the n_3-th sensor position of the third sub-array ($N_3 - 1$ sensors in

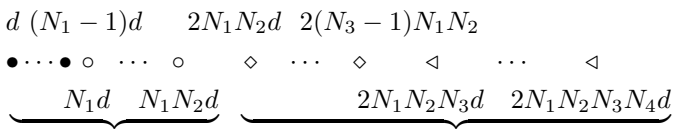

Fig. 3. A general configuration of the SE-FL-NA, consisting of four uniform linear sub-arrays, with their sensors indicated as ●, ○, ◇, and ◁, respectively.

total) and the n_4-th sensor position of the fourth sub-array (N_4 sensors in total), respectively. Again we only analyze the positive part.

For these pre-allocated sensors including the newly added zeroth sensor, the second order difference co-array lags are

$$\Phi_{\rm C}^2 = \{\mu \mid -N_1N_2 \le \mu \le N_1N_2, \mu \in \mathbb{Z}\} \ . \tag{36}$$

By calculating the cross-difference co-array between the introduced sensor and the pre-allocated sensors, the sets of consecutive integers at the fourth order difference co-array stage associated with $\alpha_{n_3}d$ and $\beta_{n_4}d$ can be expressed as

$$\begin{aligned} \phi_{\alpha_{n_3}} &= \left\{\mu \mid \nu_{\alpha_{n_3}} \le \mu \le \zeta_{\alpha_{n_3}}, \mu \in \mathbb{Z}\right\} \ , \\ \phi_{\beta_{n_4}} &= \left\{\mu \mid \nu_{\beta_{n_4}} \le \mu \le \zeta_{\beta_{n_4}}, \mu \in \mathbb{Z}\right\} \ , \end{aligned} \tag{37}$$

with

$$\begin{aligned} \nu_{\alpha_{n_3}} &= \alpha_{n_3} - 2N_1N_2, \ \ \zeta_{\alpha_{n_3}} = \alpha_{n_3} + N_1N_2 \ , \\ \nu_{\beta_{n_4}} &= \beta_{n_4} - 2N_1N_2, \ \ \zeta_{\beta_{n_4}} = \beta_{n_4} + N_1N_2 \ . \end{aligned} \tag{38}$$

Without loss of generality, we follow the same assumption that the fourth sub-array has the largest inter-element spacing, and $\beta_{n_4} > \alpha_{n_3}, \forall n_3 = 1, 2, \ldots, N_3{-}1$, $n_4 = 1, 2, \ldots, N_4$. By examining the fourth order cross-difference co-arrays between the two sub-arrays under construction, the set of consecutive lags associated with $\beta_{n_4}d - \alpha_{n_3}d$ is given by

$$\varphi_{\alpha_{n_3},\beta_{n_4}} = \left\{\mu \mid \nu_{\alpha_{n_3},\beta_{n_4}} \le \mu \le \zeta_{\alpha_{n_3},\beta_{n_4}}\right\} \ , \tag{39}$$

with the lower bound and upper bound expressed as

$$\begin{aligned} \nu_{\alpha_{n_3},\beta_{n_4}} &= \beta_{n_4} - \alpha_{n_3} - N_1N_2 \ , \\ \zeta_{\alpha_{n_3},\beta_{n_4}} &= \beta_{n_4} - \alpha_{n_3} + N_1N_2 \ . \end{aligned} \tag{40}$$

To ensure that the segments of consecutive lags $\varphi_{\alpha_{n_3},\beta_{n_4}}$ with respect to different α_{n_3} while associated with a fixed β_{n_4} are overlapped to form a larger uniform linear virtual array, the following relationship should be satisfied:

$$\zeta_{\alpha_{n_3+1},\beta_{n_4}} + 1 \ge \nu_{\alpha_{n_3},\beta_{n_4}} \ . \tag{41}$$

Then, we can obtain the inter-element spacing of the third sub-array by solving (41), given by

$$d_{N_3} = \alpha_{n_3+1} - \alpha_{n_3} \le 2N_1N_2 + 1 \ . \tag{42}$$

For simplification, we set $d_{N_3} = 2N_1N_2$ and $\alpha_1 = 2N_1N_2$. Therefore, the sensor positions of the third sub-array are

$$\alpha_{n_3}d = (\alpha_1 + (n_3 - 1)d_{N_3})\, d = 2N_1N_2n_3d \ . \tag{43}$$

Obviously, $\phi_{\beta_{n_4}}$ and $\varphi_{\alpha_1,\beta_{n_4}}$ are overlapped. As a result, $\forall n_3 = 1, 2, \ldots, N_3$, the set of consecutive integers associated with $\beta_{n_4}d$ is combined into

$$\begin{aligned} \psi_{\beta_{n_4}} &= \varphi_{\alpha_1,\beta_{n_4}} \bigcup \varphi_{\alpha_2,\beta_{n_4}} \cdots \bigcup \varphi_{\alpha_{N_3-1},\beta_{n_4}} \bigcup \phi_{\beta_{n_4}} \\ &= \left\{\mu \mid \nu_{\alpha_{N_3-1},\beta_{n_4}} \le \mu \le \zeta_{\beta_{n_4}}, \mu \in \mathbb{Z}\right\} \ . \end{aligned} \tag{44}$$

with

$$\begin{aligned} \nu_{\alpha_{N_3-1},\beta_{n_4}} &= \beta_{n_4} - \alpha_{N_3-1} - N_1N_2 \ , \\ \zeta_{\beta_{n_4}} &= \beta_{n_4} + N_1N_2 \ . \end{aligned} \tag{45}$$

To enlarge the number of consecutive lags, we can arrange the sets $\psi_{\beta_{n_4}}$ with adjacent sensors to be overlapped by ensuring

$$\nu_{\alpha_{N_3-1},\beta_{n_4+1}} \le \zeta_{\beta_{n_4}} + 1 \ , \tag{46}$$

and therefore the inter-element spacing of the fourth sub-array

$$\begin{aligned} d_{N_4} &= \beta_{n_4+1} - \beta_{n_4} \le \alpha_{N_3-1} + 2N_1N_2 + 1 \\ &= 2N_1N_2N_3 + 1 \ . \end{aligned} \tag{47}$$

We fix $d_{N_4} = 2N_1N_2N_3$, and set the first sensor in the fourth sub-array $\beta_1 = 2N_1N_2N_3$ for convenience. Then, the sensor positions of the fourth sub-array become

$$\beta_{n_4}d = [\beta_1 + (n_4 - 1)d_{N_4}]\, d = 2N_1N_2N_3n_4d \ . \tag{48}$$

The maximum integer in the set of consecutive fourth order difference co-array lags can be achieved by

$$M_{\max}^4 = \zeta_{\beta_{N_4}} = 2N_1N_2N_3N_4 + N_1N_2 \ . \tag{49}$$

Corollary 1: With the $\alpha_{n_3}d$ defined in (43), the assistant sensor at $0d$ can be removed without sacrificing the number of consecutive lags at the fourth order difference co-array stage.

Proof: See Appendix A.

As a result, the SE-FL-NA is derived and $\Phi_{\max}^4$ in (35) can be achieved by our proposed SE-FL-NA.

Remark 3: We compare $M_{\max}^4$ of the E-FL-NA in (33) by replacing N_4 with $N_4 + 1$ and the SE-FL-NA in (49) with the same sensor number $N = \sum_{m=1}^4 (N_m - 1) + 2$. The term $2N_1N_2N_3N_4$ is the largest among all terms in $M_{\max}^4$, and by applying the Arithmetic Mean-Geometric Mean (AM-GM) inequality, $2N_1N_2N_3N_4$ achieves the maximum value when $N_m = \frac{N+2}{4}$, $1 \le m \le 4$. Clearly, the ratio between $M_{\max}^4$ in (33) and (49) gets close to 1 with the increase of N, where N_m is selected as an integer around $\frac{N+2}{4}$.

B. Simplified and Enhanced Multiple Level Nested Arrays

According to *Definition 1*, the $2q$-th order difference co-array for the general linear array given in (1) is expressed as $\mathbb{C}_{2q} = \Phi_{2q} \cdot d$, where the set of the $2q$-th order difference co-array lags is given by

$$\begin{aligned} \Phi_{2q} &= \left\{ \sum_{m=1}^{q} \hbar_{n_m} - \sum_{m=q+1}^{2q} \hbar_{n_m} \right\} \\ &= \left\{ \left(\hbar_{n_q} - \hbar_{n_{2q}}\right) - \left(\sum_{m=q+1}^{2q-1} \hbar_{n_m} - \sum_{m=1}^{q-1} \hbar_{n_m} \right) \right\} \\ &= \left\{\mu_1 - \mu_2 \mid \mu_1 \in \Phi_2, \mu_2 \in \Phi_{2(q-1)}\right\} \ , \end{aligned} \tag{50}$$

where $n_m = 1, 2, \ldots, N-1$.

From this perspective, the $2q$-th order difference co-array can be obtained by calculating the difference between the virtual array at the second order difference co-array stage and the virtual array at the $2(q-1)$-th order difference co-array stage with virtual sensors in $\mathbb{C}_{2(q-1)}$.

Proposition 3: Denote $\mathbb{S}_m$ as the sensor position set of the m-th sub-array. As shown in Fig. 4, for a simplified and enhanced $2q$ level nested array (SE-$2q$L-NA, $q \geq 2$) consisting of $2q$ sub-arrays, the sets $\mathbb{S}_m$ for $m = 1, 2$ and $m = 2q$ are expressed as

$$\begin{aligned} \mathbb{S}_1 &= \{n_1 d \mid n_1 = 1, 2, \ldots, N_1 - 1\} \ , \\ \mathbb{S}_2 &= \{n_2 N_1 d \mid n_2 = 1, 2, \ldots, N_2\} \ , \\ \mathbb{S}_{2q} &= \left\{ n_{2q} 2^{q-1} \prod_{n_{2q}=1}^{2q-1} N_m d \mid n_{2q} = 1, 2, \ldots, N_{2q} \right\} \ , \end{aligned} \tag{51}$$

while $\mathbb{S}_m$ for $2 < m < 2q$, $m \in \mathbb{Z}$ with $N_m - 1$ sensors located at

$$\mathbb{S}_m = \left\{ n_m 2^{\lfloor \frac{m-1}{2} \rfloor} \prod_{n_m=1}^{m-1} N_m d \mid n_m = 1, 2, \ldots, N_m - 1 \right\} \ , \tag{52}$$

where $\lfloor x \rfloor$ returns the greatest integer that is less or equal to x. Therefore, there are $\sum_{m=1}^{2q}(N_m - 1) + 2$ sensors in total, and the set of consecutive lags at the $2q$-th order difference co-array stage is

$$\Phi_{\mathrm{C}}^{2q} = \left\{ \mu \mid -M_{\max}^{2q} \leq \mu \leq M_{\max}^{2q}, \mu \in \mathbb{Z} \right\} \ , \tag{53}$$

with $M_{\max}^{2q} = 2^{q-1} \prod_{m=1}^{2q} N_m + 2^{q-2} \prod_{m=1}^{2q-2} N_m$, and the maximum number of consecutive lags at the $2q$-th order difference co-array stage is

$$2M_{\max}^{2q} + 1 = 2^q \prod_{m=1}^{2q} N_m + 2^{q-1} \prod_{m=1}^{2q-2} N_m + 1 \ . \tag{54}$$

Proof: Obviously, the SE-FL-NAs is obtained when $q = 2$. For $q > 2$, assume that the set of consecutive lags included at the $2(q-1)$-th difference co-array stage of the derived SE-$2(q-1)$L-NA can be expressed as

$$\Phi_{\mathrm{C}}^{2(q-1)} = \left\{ \mu \mid -M_{2(q-1)} \leq \mu \leq M_{2(q-1)}, \mu \in \mathbb{Z} \right\} \ , \tag{55}$$

where $M_{2(q-1)} \leq M_{\max}^{2(q-1)}$ is a selected positive number of the consecutive $2(q-1)$-th order difference co-array lags, with the purpose of both enlarging the length of the consecutive co-arrays of the enhanced array configuration and simplifying the formulations of the sensor positions.

The optimum configuration of the SE-$2q$L-NA can be obtained by constructing two extra sub-arrays based on a given SE-$2(q-1)$L-NA. Denote $N_{2q-1} - 1$ and N_{2q} as the sensor number of the $(2q-1)$-th sub-array and the $2q$-th sub-array under construction, with $\alpha_{n_{2q-1}} d$, $n_{2q-1} = 1, 2, \ldots, N_{2q-1}$, and $\beta_{n_{2q}} d$, $n_2 q = 1, 2, \ldots, N_{2q}$, representing the n_{2q-1}-th and the n_{2q}-th sensor position of the $(2q-1)$-th sub-array and the the $2q$-th sub-array, respectively. Again due to the symmetry, we only consider optimizing the positive co-array lags.

Following the same approach, a sensor at the zeroth position is added first. Then, the cross-difference co-array between the introduced sensor and the pre-allocated sensors is given by

$$\begin{aligned} \phi_{\alpha_{n_{2q-1}}} &= \left\{ \mu \mid \nu_{\alpha_{n_{2q-1}}} \leq \mu \leq \zeta_{\alpha_{n_{2q-1}}}, \mu \in \mathbb{Z} \right\} \ , \\ \phi_{\beta_{n_{2q}}} &= \left\{ \mu \mid \nu_{\beta_{n_{2q}}} \leq \mu \leq \zeta_{\beta_{n_{2q}}}, \mu \in \mathbb{Z} \right\} \ , \end{aligned} \tag{56}$$

where the lower and upper bounds are

$$\begin{aligned} \nu_{\alpha_{n_{2q-1}}} &= \alpha_{n_{2q-1}} - \hbar_{\max}^{2(q-1)} - M_{2(q-1)} \ , \\ \zeta_{\alpha_{n_{2q-1}}} &= \alpha_{n_{2q-1}} + M_{2(q-1)} \ , \\ \nu_{\beta_{n_{2q}}} &= \beta_{n_{2q}} - \hbar_{\max}^{2(q-1)} - M_{2(q-1)} \ , \\ \zeta_{\beta_{n_{2q}}} &= \beta_{n_{2q}} + M_{2(q-1)} \ . \end{aligned} \tag{57}$$

with $\hbar_{\max}^{2(q-1)} d$ being the maximum physical array sensor position in the pre-designed SE-$2(q-1)$L-NA.

Denote $\hbar_q^{n_q}$ as the n_q-th sensor in the q-th sub-array, and N_q is the number of sensors of the corresponding sub-array. Without loss of generality, large sensor positions are assigned to higher level sub-arrays with $\hbar_{q_1}^{n_{q_1}} > \hbar_{q_2}^{n_{q_2}}$, $\forall n_{q_1} = 1, 2, \ldots, N_{q_1}$, $n_{q_2} = 1, 2, \ldots, N_{q_2}$ when $q_1 > q_2$. By examining the cross-difference co-arrays between the two extra sub-arrays, the consecutive lags associated with $\beta_{n_{2q}} d - \alpha_{n_{2q-1}} d$ are given by

$$\begin{aligned} &\varphi_{\alpha_{n_{2q-1}}, \beta_{n_{2q}}} \\ &= \left\{ \mu \mid \nu_{\alpha_{n_{2q-1}}, \beta_{n_{2q}}} \leq \mu \leq \zeta_{\alpha_{n_{2q-1}}, \beta_{n_{2q}}}, \mu \in \mathbb{Z} \right\} \ , \end{aligned} \tag{58}$$

where

$$\begin{aligned} \nu_{\alpha_{n_{2q-1}}, \beta_{n_{2q}}} &= \beta_{n_{2q}} - \alpha_{n_{2q-1}} - M_{2(q-1)} \ , \\ \zeta_{\alpha_{n_{2q-1}}, \beta_{n_{2q}}} &= \beta_{n_{2q}} - \alpha_{n_{2q-1}} + M_{2(q-1)} \ . \end{aligned} \tag{59}$$

For a fixed $\beta_{n_{2q}}$, the segments of consecutive lags $\varphi_{\alpha_{n_{2q-1}}, \beta_{n_{2q}}}$ with respect to $\alpha_{n_{2q-1}}$ are designed to be overlapped to form a larger uniform linear virtual array at the $2q$-th order difference co-array stage, satisfying

$$\zeta_{\alpha_{n_{2q-1}+1}, \beta_{n_{2q}}} + 1 \geq \nu_{\alpha_{n_{2q-1}}, \beta_{n_{2q}}} \ . \tag{60}$$

By solving (60), the inter-element spacing of the $2q-1$-th sub-array is obtained, given by

$$d_{N_{2q-1}} = \alpha_{n_{2q-1}+1} - \alpha_{n_{2q-1}} \leq 2M_{2(q-1)} + 1 \ . \tag{61}$$

To simplify the formulations, we fix $d_{N_{2q-1}}$ and the location of its first sensor $\alpha_1 d$ as

$$d_{N_{2q-1}} = 2M_{2(q-1)} \ , \quad \alpha_1 d = 2M_{2(q-1)} d \ , \tag{62}$$

and therefore the sensor positions of the constructed $2q-1$-th sub-array are expressed as

$$\begin{aligned} \alpha_{n_{2q-1}} d &= \left[\alpha_1 + (n_{2q-1} - 1) d_{N_{2q-1}} \right] d \\ &= 2M_{2(q-1)} n_{2q-1} d \ , \end{aligned} \tag{63}$$

where $n_{2q-1} = 1, 2, \ldots, N_{2q-1} - 1$.

According to (63), $\phi_{\beta_{n_{2q}}}$ and $\varphi_{\alpha_1, \beta_{n_{2q}}}$ are overlapped. Then, the set of consecutive integers at the $2q$-th order difference co-array stage is

$$\begin{aligned} \psi_{\beta_{n_{2q}}} &= \varphi_{\alpha_1, \beta_{n_{2q}}} \bigcup \varphi_{\alpha_2, \beta_{n_{2q}}} \ldots \bigcup \varphi_{\alpha_{N_{2q-1}-1}, \beta_{n_{2q}}} \bigcup \phi_{\beta_{n_{2q}}} \\ &= \left\{ \mu \mid \nu_{\alpha_{N_{2q-1}-1}, \beta_{n_{2q}}} \leq \mu \leq \zeta_{\beta_{n_{2q}}} \right\} \ . \end{aligned}$$

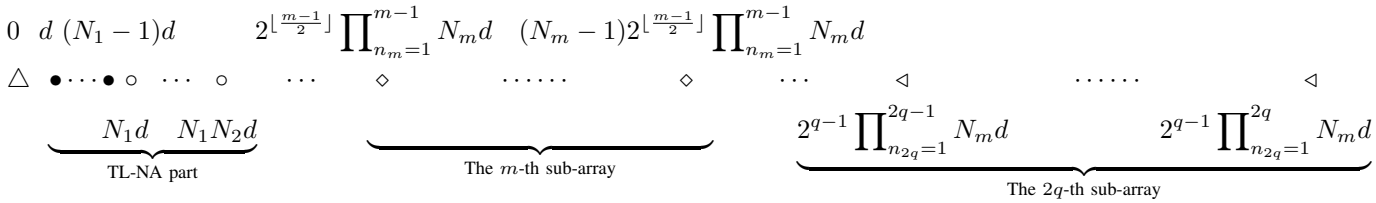

Fig. 4. A general configuration of the SE-2qL-NA, consisting of $2q$ uniform linear sub-arrays. Note that the assistant sensor $\triangle$ at the zeroth position is finally removed from our proposed configuration.

with

$$\begin{aligned} \nu_{\alpha_{N_{2q-1}-1},\beta_{n_{2q}}} &= \beta_{n_{2q}} - \alpha_{N_{2q-1}-1} - M_{2(q-1)} \ , \\ \zeta_{\beta_{n_{2q}}} &= \beta_{n_{2q}} + M_{2(q-1)} \ . \end{aligned} \tag{64}$$

To ensure the segments of consecutive lags in $\psi_{\beta_{n_{2q}}}$ with adjacent n_{2q} are overlapped, the sensors of the $2q$-th sub-array should satisfy the following relationship:

$$\nu_{\alpha_{N_{2q-1}-1},\beta_{n_{2q}+1}} \leq \zeta_{\beta_{n_{2q}}} + 1 \ . \tag{65}$$

Then we can obtain the inter-element spacing of the $2q$-th sub-array, given by

$$\begin{aligned} d_{N_{2q}} &= \beta_{n_{2q}+1} - \beta_{n_{2q}} \leq \alpha_{N_{2q-1}-1} + 2M_{2(q-1)} + 1 \\ &= 2M_{2(q-1)}N_{2q-1} + 1 \ . \end{aligned} \tag{66}$$

We set $d_{N_{2q}} = 2M_{2(q-1)}N_{2q-1}$, and $\beta_1 = 2M_{2(q-1)}N_{2q-1}$ for simplification of the location formulations. The sensor positions of the $2q$-th sub-array can then be expressed as

$$\begin{aligned} \beta_{n_{2q}} d &= \left[2M_{2(q-1)}N_{2q-1} + (n_{2q}-1)d_{N_{2q}}\right] d \\ &= 2M_{2(q-1)}N_{2q-1}n_{2q}d \ , \end{aligned} \tag{67}$$

where $n_{2q} = 1, 2, \ldots, N_{2q}$, and the maximum integer in the set of consecutive lags at the $2q$-th order difference co-array stage reaches

$$M_{\max}^{2q} = \zeta_{\beta_{N_{2q}}} = 2M_{2(q-1)}N_{2q-1}N_{2q} + M_{2(q-1)} \ . \tag{68}$$

We can set $M_{2q} = M_{\max}^{2q}$ to design the two extra introduced sub-arrays. However, for convenience of sensor position formulations of each sub-array in SE-2qL-NA, we select $M_{2q} = 2M_{2(q-1)}N_{2q-1}N_{2q}$ by sacrificing some potential DOFs provided by the constructed SE-2qL-NA, and therefore

$$\frac{M_{2q}}{M_{2(q-1)}} = 2N_{2q-1}N_{2q} \ . \tag{69}$$

Based on *Proposition 2* for SE-FL-NA and (69), we obtain

$$M_{2q} = 2^{q-1}\prod_{m=1}^{2q} N_m \ . \tag{70}$$

Then the sensor positions of the introduced two sub-arrays can be expressed as

$$\begin{aligned} \alpha_{n_{2q-1}} d &= 2^{q-1}\prod_{m=1}^{2q-2} N_m n_{2q-1} d \ , \\ \beta n_{2q} d &= 2^{q-1}\prod_{m=1}^{2q-1} N_m n_{2q} d \ . \end{aligned} \tag{71}$$

Corollary 2: With the defined $\alpha_{n_{2q-1}}d$, the assistant sensor at $0d$ can be removed without sacrificing the number of consecutive lags at the $2q$-th order difference co-array stage.

Proof: See Appendix B.

According to (62) and (67), it is noted that $\alpha_1 = 2M_{2(q-1)} = 2M_{2(q-2)}N_{2q-3}N_{2q-2}$, which means that the first sensor in the $(2q-1)$-th sub-array is shared with the last sensor (the N_{2q-2}-th sensor) in the $(2q-2)$-th sub-array. As a result, the sensor positions of all sub-arrays in SE-2qL-NA ($q \geq 2$) can be derived, where the sets $\mathbb{S}_m$ for $m = 1, 2, \ldots, 2q$ are expressed in (51) and (52).

According to (68), it is obvious that $M_{\max}^{2q} = 2^{q-1}\prod_{m=1}^{2q} N_m + 2^{q-2}\prod_{m=1}^{2q-2} N_m$, and then the maximum number of consecutive lags at the $2q$-th order difference co-array stage is $2M_{\max}^{2q} + 1$.

Remark 4-(1): Different from all the virtual arrays at higher order difference co-array stage, the physical array does not share the symmetric property. After selecting an appropriate inter-element spacing, the first sensor location in each sub-array is defined to be equal to the corresponding inter-element spacing, leading to the simplified and enhanced multiple level nested array (SE-ML-NA).

Remark 4-(2): The sensor position formulations of the SE-ML-NA in (51) and (52) are simple, and each formulation is independent of the virtual ULA apertures at the lower order difference co-array stage. As a result, the SE-ML-NA is far more comprehensive and also convenient for structure construction.

V. Comparison of DOFs and Simulation Results

For all simulations, we set $d = \lambda/2$. After combining the redundant co-arrays together [28], SS-MUSIC is employed for DOA estimation, and all the K source signals are uniformly distributed between -60° and 60°.

A. Comparison and DOA Estimation Results for Configurations Based on the Fourth Order Difference Co-Array

We first focus on the performances of a series of nested configurations where the standard TL-NA is employed as part of the array structure, i.e., FL-NA, SAFOE-NA, EAS-NA-NA, and the proposed E-FL-NA. Then, further comparison between the E-FL-NA and the 2L-FO-NA will be given in *3)*.

1) Comparison in the Number of DOFs

For N given physical sensors, more DOFs can be provided by the proposed E-FL-NA compared with the FL-NA and the SAFOE-NA due to the larger inter-element spacing in the third sub-array and the fourth sub-array. As analyzed in [44], the EAS-NA-NA is capable of resolving more sources than the SAFOE-NA and FL-NA with the same number of sensors. For comparison between our proposed E-FL-NA and the EAS-NA-NA, we have the following corollary:

TABLE I
COMPARISON OF THE CONSECUTIVE LAGS FOR DIFFERENT ARRAY STRUCTURES BASED ON THE FOURTH ORDER DIFFERENCE CO-ARRAYS

Array Structures	Number of Sensors	Number of Consecutive Fourth Order Difference Co-Array Lags
FL-NA	$\sum_{m=1}^{4}(N_m-1)+1$	$2N_1N_2N_3(N_4+1)-1$
SAFOE-NA	$\sum_{m=1}^{3}(N_m-1)+1$	$2(3N_3-1)N_1N_2-4N_3+1$
EAS-NA-NA	$\sum_{m=1}^{3}(N_m-1)+1$	$M_{\text{EAS}}{}^{\dagger}$
E-FL-NA	$\sum_{m=1}^{4}(N_m-1)+1$	$M_{\text{E}}{}^{\ddagger}$
Examples of different structures for comparison		
Array Structures	$(N_1,\ldots,N_m)$ $2\le m\le 4$	Number of Sensors / Number of Consecutive Lags
FL-NA	$(2,2,2,3)$	6 / 63
SAFOE-NA	$(2,3,3)$	6 / 85
EAS-NA-NA	$(2,2,2,3)$	6 / 83
E-FL-NA	$(2,2,2,3)$	6 / 95
FL-NA	$(3,3,3,3)$	9 / 215
SAFOE-NA	$(3,4,4)$	9 / 249
EAS-NA-NA	$(3,3,3,3)$	9 / 305
E-FL-NA	$(3,3,3,3)$	9 / 337
FL-NA	$(3,4,4,4)$	12 / 479
SAFOE-NA	$(4,5,5)$	12 / 541
EAS-NA-NA	$(3,4,4,4)$	12 / 735
E-FL-NA	$(3,4,4,4)$	12 / 801

† $M_{\text{EAS}}=(2N_1N_2-1)(2N_3N_4-1)+2(N_1N_2-1)$.
‡ $M_{\text{E}}=2N_3N_4(2N_1N_2-1)+2(N_4-1)(N_1N_2-1)-1$.

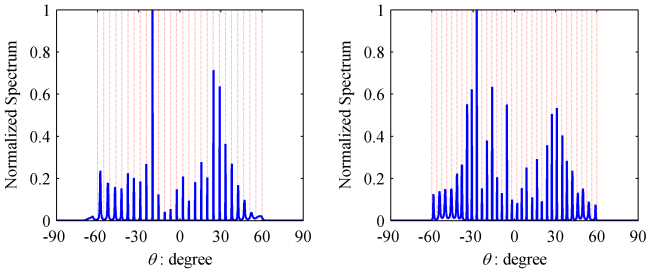

(a) FL-NA ($K=28$). (b) SAFOE-NA ($K=34$).

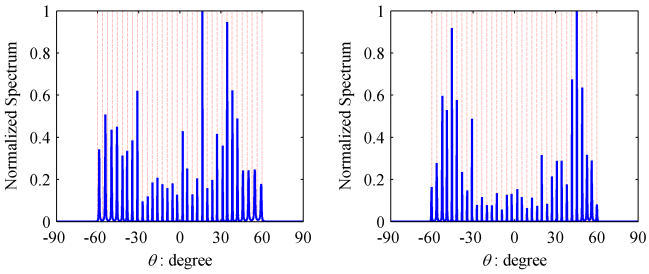

(c) EAS-NA-NA ($K=34$). (d) E-NA-NA ($K=34$).

Fig. 5. DOA estimation results for different array configurations based on the fourth order difference co-array.

Corollary 3: Given the same number of physical sensors, the potential DOFs provided by an optimized E-FL-NA can be more than any configurations of EAS-NA-NA [44].

Proof: For an EAS-NA-NA with $\prod_{m=1}^{4}(N_m-1)+1$ sensors, its number of consecutive co-array lags at the fourth order difference co-array stage is $M_{\text{EAS}}=(2N_1N_2-1)(2N_3N_4-1)+2(N_1N_2-1)$. However, for E-FL-NA, this number is $M_{\text{E}}=2N_3N_4(2N_1N_2-1)+2(N_4-1)(N_1N_2-1)-1$. The difference between the two for the same (N_1,N_2,N_3,N_4) is

$$\Delta M_4=M_{\text{E}}-M_{\text{EAS}}=2(N_4-1)(N_1N_2-1)>0\,. \quad (72)$$

To ensure the existence of each level, $N_4\ge 2$.

As a result, there always exists a configuration in E-FL-NA which can provide more DOFs than any EAS-NA-NA. As shown in (30), the inter-element spacing in the fourth sub-array of an E-FL-NA is $N_3(2N_1N_2-1)+N_1N_2-1$. The physical aperture N_1N_2-1 is not exploited in the EAS-NA-NA, and thus E-FL-NA is a better configuration for the fourth order difference co-array enhancement.

The number of consecutive integers at the fourth order difference co-array stage for different structures is listed in Table I. It is clear that with a larger inter-element spacing in the third and fourth sub-arrays, the DOFs provided by the E-FL-NA is much more than that of an FL-NA with the same N_m, $m=1,2,3,4$. Combined with *Corollary 3*, with a fixed number of sensors, E-FL-NA is the best one offering the largest number of consecutive lags among all those configurations for the fourth order difference co-array enhancement.

2) DOA Estimation Results

Now consider examples with $N=6$ physical sensors: $(2,2,2,3)$ for FL-NA, $(2,3,3)$ for SAFOE-NA, $(2,2,2,3)$ for EAS-NA-NA, and $(2,2,2,3)$ for E-FL-NA.

For the first set of simulations, the SNR is set to be 20 dB. To evaluate the number of distinguishable sources, a sufficient number of snapshots for calculating the fourth order cumulant matrix is used, fixed at 500000, and different number of sources K is used for different configurations. The DOA estimation results for different array configurations are shown in Fig. 5, where the dotted lines represent the actual incident angles of the impinging signals, whereas the solid lines represent the estimation results. It is clear that FL-NA, SAFOE-NA and EAS-NA-NA have failed in resolving all the 28, 34, and 34 sources respectively, while the proposed E-FL-NA has resolved the 34 sources successfully.

In the second set of simulations, we focus on the root mean square error (RMSE) results to compare the estimation accuracy of different array configurations through Monte Carlo simulations of 500 trials. The number of sources K is 10. Fig. 6(a) gives the results with respect to a varied input SNR, where the number of snapshots is fixed at 10000. Clearly, the performance of E-FL-NA is the best, with that of the FL-NA being the worst. It is noted that the physical aperture for E-FL-NA is $44d$, while it is $23d$ for FL-NA, $37d$ for SAFOE-NA, and $38d$ for EAS-NA-NA. With the largest aperture in both physical array and virtual array, the proposed configuration has consistently outperformed the other three.

In Fig. 6(b), the RMSE results with respect to different number of snapshots are shown, where SNR is fixed at 0 dB. Due to a better estimation of the statistics of the involved signals, the larger the number of snapshots, the higher its estimation accuracy. Similarly, the performance of the proposed E-FL-NA is still the best among them.

3) E-FL-NA versus 2L-FO-NA

The 2L-FO-NA structure in [45] consists of two sub-arrays

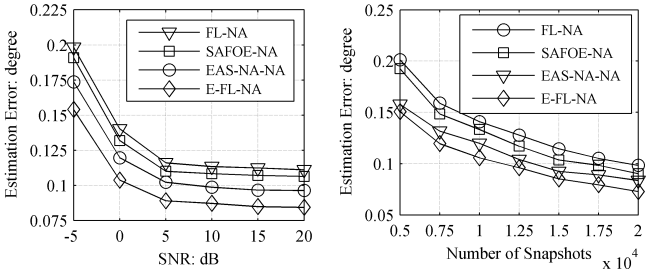

(a) RMSE results versus input SNR. (b) RMSE results versus number of snapshots.

Fig. 6. RMSE results of different array configurations.

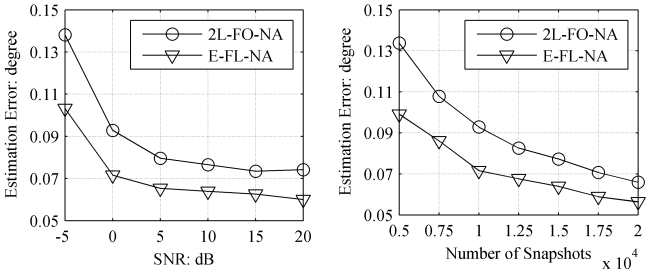

(a) RMSE results versus input SNR. (b) RMSE results versus number of snapshots.

Fig. 8. RMSE results of the E-FL-NA and the 2L-FO-NA.

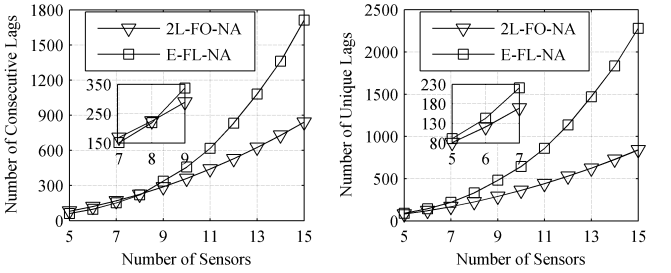

(a) Number of consecutive lags versus number of sensors. (b) Number of unique lags versus number of sensors.

Fig. 7. Number of consecutive and unique lags of different configurations with respect to the number of physical sensors.

with N_1 sensors and N_2 sensors respectively, and it is a specially designed hole-free configuration with respect to the consecutive fourth order difference co-array lags where a number of $16N_1N_2 - 8N_2 + 1$ lags is achieved. As illustrated in [45], when the number of sensors $N < 12$, the 2L-FO-NA offers higher number of consecutive fourth order difference co-array lags compared with SAFOE-NA [42]; otherwise more DOFs are provided by SAFOE-NA.

As demonstrated earlier, the proposed E-FL-NA outperforms the SAFOE-NA. Therefore, we further compare the number of consecutive fourth order difference co-array lags of E-FL-NA and 2L-FO-NA versus the number of physical sensors, as shown in Fig. 7(a), where each point is the maximum number of consecutive lags among all potential configurations. We can see clearly that higher number of the consecutive fourth order difference co-array lags can be achieved by our proposed E-FL-NA when the sensor number $N \geq 9$.

On the other hand, as shown in *Remark 1*, we minimize the redundancies introduced by each additional sensor under construction based on a standard TL-NA with certain redundancies, and therefore both the consecutive lags and the unique lags are increased. However, the TL-NA is not part of the 2L-FO-NA. Then, we compare the unique fourth order lags of the two configurations using the same structure analyzed in Fig. 7(a), and the results are given in Fig. 7(b). Obviously, the number of unique lags of the proposed E-FL-NA exceeds that of the 2L-FO-NA for any number of sensors.

Finally, we fix the number of sensors to 6, and the CS-based method utilizing all unique lags is applied based on the structures offering the largest number of lags in Fig. 7, i.e., E-FL-NA with $(2, 2, 2, 3)$ and 2L-FO-NA with $(3, 3)$. Fig. 8(a) shows the RMSE results with respect to the input SNR, while Fig. 8(b) gives the RMSE results with repect to the number of snapshots. It is clear that the E-FL-NA with larger number of unique lags outperforms the 2L-FO-NA due to its larger physical and virtual array aperture.

B. Comparison and DOA Estimation Results for Configurations based on High Order Difference Co-Array

1) SE-ML-NA versus ML-NA

For array configurations with the $2q$-th order difference co-array enhancement, there are N_2 sensors in the second sub-array of a SE-$2q$L-NA, while $N_2 - 1$ sensors are included in the second sub-array of a $2q$L-NA.

Corollary 4: With the same number of physical sensors, the potential DOFs provided by an optimized SE-$2q$L-NA can be more than any configurations of $2q$L-NA if N_{2q} satisfies

$$N_{2q} \geq \begin{cases} 3, & q = 2\,, \\ 2, & q > 2\,. \end{cases} \tag{73}$$

Proof: For comparison with a $2q$L-NA, whose number of consecutive lags at the $2q$-th order difference co-array stage reaches $M_{\text{ML}} = 2(\prod_{m=1}^{2q} N_m + \prod_{m=1}^{2q-1} N_m) - 1 = 2(N_{2q}+1)\prod_{m=1}^{2q-1} N_m - 1$ with $\sum_{m=1}^{2} q(N_m - 1) + 1$ sensors, we remove the last sensor in the $2q$-th sub-array of a SE-$2q$L-NA, and therefore with the same $\sum_{m=1}^{2} q(N_m - 1) + 1$ physical sensors, its number of consecutive lags arrives at $M_{\text{SE}} = 2^q \prod_{m=1}^{2q-1} N_m(N_{2q} - 1) + 2^{q-1} \prod_{m=1}^{2q-2} N_m + 1$. Then the difference between the two is

$$\begin{aligned} \Delta M &= M_{\text{SE}} - M_{\text{ML}} \\ &= \prod_{m=1}^{2q-1} N_m \left[(2^q - 2)N_{2q} - (2^q + 2)\right] + 2^{q-1} \prod_{m=1}^{2q-2} N_m + 2\,. \end{aligned}$$

Clearly, the second term $2^{q-1} \prod_{m=1}^{2q-2} N_m > 0$. After removing the last sensor in SE-$2q$L-NA, the $2q$-th level sub-array has $N_{2q} - 1$ sensors. To ensure the existence of each level, N_{2q} should satisfy $N_{2q} \geq 2$. By forcing the first term $\prod_{m=1}^{2q-1} N_m \left[(2^q - 2)N_{2q} - (2^q + 2)\right] \geq 0$, we obtain

$$N_{2q} \geq \begin{cases} \dfrac{2^q + 2}{2^q - 2} = 3, & q = 2\,, \\ \dfrac{2^q + 2}{2^q - 2} \geq 2, & q > 2\,. \end{cases} \tag{74}$$

TABLE II
COMPARISON OF THE CONSECUTIVE LAGS FOR DIFFERENT ARRAY STRUCTURES BASED ON THE $2q$-TH ORDER DIFFERENCE CO-ARRAYS

Array Structures	Number of Sensors	Number of Consecutive Co-Array Lags
$2q$L-NA	$\sum_{m=1}^{2q}(N_m-1)+1$	$2(N_{2q}+1)\prod_{m=1}^{2q-1}N_m-1$
SE-$2q$L-NA	$\sum_{m=1}^{2q}(N_m-1)+2$	M_{SE}[†]
Examples of different structures for $q=2$		
Array Structures	$(N_1,\ldots,N_{2q})$ $q=2$	Number of Sensors	Number of Consecutive Lags
FL-NA	$(2,2,2,3)$	6	63
SE-FL-NA	$(2,2,2,2)$	6	73
FL-NA	$(3,4,4,4)$	12	479
SE-FL-NA	$(3,4,4,3)$	12	601
Examples of different structures for $q=3$			
Array Structures	$(N_1,\ldots,N_{2q})$ $q=3$	Number of Sensors	Number of Consecutive Lags
6L-NA	$(2,2,2,2,2,2)$	7	191
SE-6L-NA	$(2,2,2,2,2,1)$	7	321
6L-NA	$(2,3,3,3,3,3)$	12	1295
SE-6L-NA	$(2,3,3,3,3,2)$	12	2809

[†] $M_{\text{SE}}=2^q\prod_{m=1}^{2q}N_m+2^{q-1}\prod_{m=1}^{2q-2}N_m+1$.

Then for N_{2q} satisfying (74), we have

$$\Delta M = M_{\text{SE}} - M_{\text{ML}} > 0\ . \tag{75}$$

2) DOA Estimation Results for SE-ML-NA and ML-NA

For SE-ML-NA and ML-NA, the number of consecutive integers at the $2q$-th order difference co-array stage is listed in Table II. With a fixed number of sensors, the number of consecutive co-array lags of SE-$2q$L-NA is much more than that of $2q$L-NA.

The optimal sensor allocation for a $2q$L-NA is given in *Corollary 3* in [39]. With the optimal N_m, $m=1,2,\ldots,2q$, the number of sensors in $2q$L-NA is $N=\sum_{m=1}^{2q}(N_m-1)+1$. Then we set the same N_m, $m=1,2,\ldots,2q-1$, for the corresponding sub-arrays of the proposed SE-$2q$L-NA, while $N_{2q}-1$ sensors are allocated to the last sub-array to ensure that the number of sensors achieves the same N as the $2q$L-NA. Based on this, the number of consecutive lags at the fourth order stage for SE-$2q$L-NA and $2q$L-NA ($q=2$) is shown in Fig. 9(a), where we can see that the number of consecutive co-array lags increases significantly with the number of sensors for the same configuration, while more consecutive lags can be provided by SE-$2q$L-NA with a fixed N.

Next we analyze the number of consecutive co-array lags at the $2q$-th order stage with respect to a varied order q, as shown in Fig. 9(b), where the number of sensors is fixed to $N=25$ and the optimal sensor allocation is adpted. As expected, an extremely high number of consecutive lags can be achieved by SE-$2q$L-NA compared with $2q$L-NA for a fixed q, and for the same configuration, the larger the number of q, the higher its number of consecutive lags.

To analyze the number of distinguishable sources, we set $q=2$, and the input SNR is 20 dB. The number of snapshots is 500000. The DOA estimation results for SE-$2q$L-NA ($q=2$) are shown in Fig. 10. Obviously, under the same situation, SE-$2q$L-NA is capable of resolving all the 28 sources successfully,

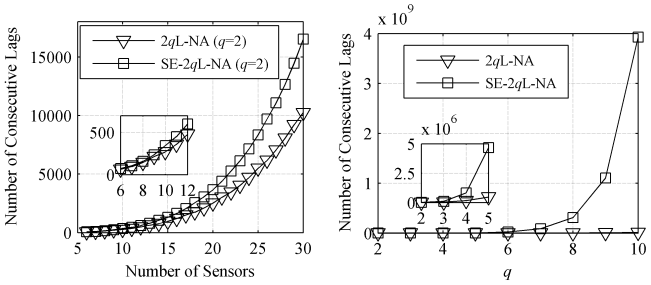

(a) Number of consecutive lags versus number of sensors. (b) Number of consecutive lags versus order q.

Fig. 9. Number of consecutive lags of different configurations.

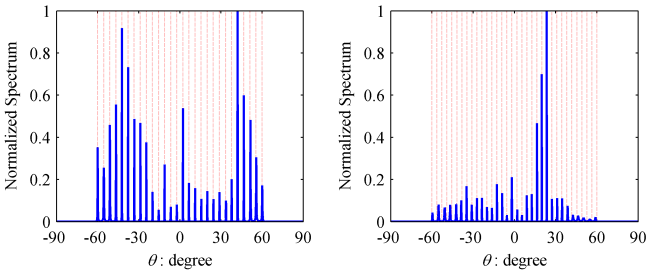

(a) Results for SE-$2q$L-NA ($K=28$). (b) Results for SE-$2q$L-NA ($K=34$).

Fig. 10. DOA estimation results for SE-$2q$L-NA ($q=2$) with different number of sources.

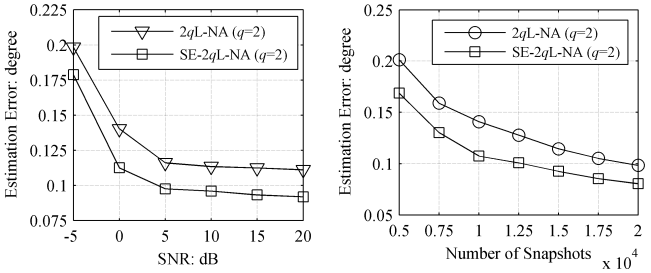

(a) RMSE results versus SNR. (b) RMSE results versus number of snapshots.

Fig. 11. Number of consecutive lags of different configurations.

while $2q$L-NA ($q=2$) fails as already given in Fig. 5(a). However, SE-$2q$L-NA ($q=2$) is unable to detect 34 sources, and therefore its resolution is worse than E-FL-NA in Fig. 5(d) due to the compromise of potential DOFs in array configuration for simplification.

Then we compare the estimation accuracy of SE-$2q$L-NA and $2q$L-NA ($q=2$), through Monte Carlo simulations of 500 trials. we set the number of sources $K=10$, and the number of snapshots is 10000. The RMSE results with respect to a varied input SNR are shown in Fig. 11(a). With a larger physical array aperture of $31d$ for the proposed SE-$2q$L-NA compared with $23d$ for $2q$L-NA and also a larger virtual ULA aperture corresponding to Table II and Fig. 9(a), the proposed SE-$2q$L-NA ($q=2$) consistently outperforms $2q$L-NA ($q=2$) by a large margin.

The RMSE results versus the different number of snapshots are shown in Fig. 11(b), where the input SNR is set to 0 dB,

$K = 10$, $q = 2$, and the number of snapshots is 10000. Clearly, these RMSE results again verifies the superior performance of the proposed SE-2qL-NA.

VI. Conclusion

The fourth order difference co-array construction problem has been investigated with a novel enhanced four level nested array (E-FL-NA) proposed at first based on the fourth order co-array concept with a significant increase in DOFs. This new configuration is then simplified, leading to a simplified and enhanced array structure SE-FL-NA, which is finally extended to form the array structure SE-2qL-NA with $2q$ uniform linear sub-arrays by optimizing the consecutive co-array lags at the $2q$-th order difference co-array stage. It has been shown by simulations that among all considered array configurations, the proposed E-FL-NA can resolve most sources, and a better performance can be achieved due to its larger physical and virtual array aperture. Furthermore, with a fixed number of sensors, the proposed SE-ML-NA offers many more DOFs than the ML-NA, especially for a larger q, and therefore superior performances including more resolvable sources and more accurate estimation results have been achieved.

Appendix A
Proof of the Corollary 1

After removing the zeroth sensor at $0d$, the sets of the positive cross-difference co-array lags between the introduced sensors and the pre-allocated sensors are the same as those in (19) and (20), with the consecutive second order difference co-array lags expressed as $\Phi_{\rm C}^2 = \{\mu, -N_1N_2+1 \le \mu \le N_1N_2-1, \mu \in \mathbb{Z}\}$. However, by considering $\alpha_1 d = 2N_1N_2 d$ in the constructed SE-FL-NA as one of the pre-allocated sensor, an extra co-array lag of $2N_1N_2 - N_1N_2 = N_1N_2$ can be acquired at the second order difference co-array stage, and therefore $\Phi_{\rm C}^2$ is updated to $\Phi_{\rm C}^2 = \{\mu, -N_1N_2 \le \mu \le N_1N_2\}$, which is the same as in (36). As a result, (19) and (20) change to

$$\begin{aligned} \phi_{\alpha_{n_3}} &= \left\{\mu \mid \nu_{\alpha_{n_3}} \le \mu \le \zeta_{\alpha_{n_3}}, \mu \in \mathbb{Z}\right\} , \\ \phi_{\beta_{n_4}} &= \left\{\mu \mid \nu_{\beta_{n_4}} \le \mu \le \zeta_{\beta_{n_4}}, \mu \in \mathbb{Z}\right\} , \end{aligned} \tag{76}$$

where

$$\begin{aligned} \nu_{\alpha_{n_3}} &= \alpha_{n_3} - 2N_1N_2 , \quad \zeta_{\alpha_{n_3}} = \alpha_{n_3} - 1 + N_1N_2 , \\ \nu_{\beta_{n_4}} &= \beta_{n_4} - 2N_1N_2 , \quad \zeta_{\beta_{n_4}} = \beta_{n_4} - 1 + N_1N_2 . \end{aligned} \tag{77}$$

Furthermore, a discrete value of $\alpha_{n_3} + N_1N_2 = \alpha_{n_3} + \alpha_1 - aN_2 - bN_2$ and $\beta_{n_3} + N_1N_2 = \beta_{n_3} + \alpha_1 - aN_2 - bN_2$ can be achieved when $a + b = N_1$, $a, b = 1, 2, \ldots, N_1 - 1$. Clearly, $aN_2 \cdot d, bN_2 \cdot d \in \mathbb{S}_2$. Therefore, the upper and lower bounds in (77) are finally the same as those in (38).

Then we can derive the sensor positions of the two extra sub-arrays as shown in (43) and (48), leading to the proposed SE-FL-NA given in (34), and the same maximum integer in the set of consecutive fourth order difference co-array lags $M_{\max}^4$ can be obtained.

Remark A: Note that for SAFOE-NAs in [42] and E-FL-NAs in Section III-B, the consecutive lags are maximised with a displacement equal to the inter-element spacing between the starting sensor of the constructed sub-array and the last sensor of a lower level sub-array. Therefore, the co-array segments or discrete values associated with their $\alpha_1 d$ and $\beta_1 d$ are unable to be considered as one overlapped part in the array construction.

Appendix B
Proof of the Corollary 2

After removing the zeroth sensor at $0d$, we still assume that the set of consecutive lags included at the $2(q-1)$-th difference co-array stage of the derived SE-2$(q-1)$L-NA is illustrated in (55).

By constructing two sub-arrays simultaneously, the positive part of the cross-difference co-array lags between the introduced sensor and the pre-allocated sensors is given by

$$\begin{aligned} \phi_{\alpha_{n_{2q-1}}} &= \left\{\mu \mid \nu_{\alpha_{n_{2q-1}}} \le \mu \le \zeta_{\alpha_{n_{2q-1}}}, \mu \in \mathbb{Z}\right\} , \\ \phi_{\beta_{n_{2q}}} &= \left\{\mu \mid \nu_{\beta_{n_{2q}}} \le \mu \le \zeta_{\beta_{n_{2q}}}, \mu \in \mathbb{Z}\right\} , \end{aligned} \tag{78}$$

where the lower and upper bounds are given by

$$\begin{aligned} \nu_{\alpha_{n_{2q-1}}} &= \alpha_{n_{2q-1}} - \hbar_{\max}^{2(q-1)} - M_{2(q-1)} , \\ \zeta_{\alpha_{n_{2q-1}}} &= \alpha_{n_{2q-1}} - \hbar_{\min}^{2(q-1)} + M_{2(q-1)} , \\ \nu_{\beta_{n_{2q}}} &= \beta_{n_{2q}} - \hbar_{\max}^{2(q-1)} - M_{2(q-1)} , \\ \zeta_{\beta_{n_{2q}}} &= \beta_{n_{2q}} - \hbar_{\min}^{2(q-1)} + M_{2(q-1)} . \end{aligned} \tag{79}$$

with $\hbar_{\max}^{2(q-1)} d$ being the maximum physical array position in the pre-designed SE-2$(q-1)$L-NA, while $\hbar_{\min}^{2(q-1)} d$ represents the minimum physical array position in the corresponding array configuration. Note that $\hbar_{\min}^{2(q-1)} d = 1d$ after removing the zeroth sensor.

According to (67), the sensor position set of the $(2q-2)$-th level sub-array is

$$\mathbb{S}_{2(q-1)} = \left\{2M_{2(q-2)}N_{2q-3}n_{2q-2}d\right\} , \tag{80}$$

where $n_{2q-2} = 1, 2, \ldots, N_{2q-2} - 1$.

With a given $\alpha_1 d = 2M_{2(q-1)}d$ in (62) and $M_{2(q-1)} = 2M_{2(q-2)}N_{2q-3}N_{2q-2}$ in (69), we can figure out that the co-array lag $\alpha_{n_{2q-1}} + M_{2(q-1)} = \alpha_{n_{2q-1}} + \alpha_1 - a \cdot 2M_{2(q-2)}N_{2q-3} - b \cdot 2M_{2(q-2)}N_{2q-3}$ and $\beta_{n_{2q-1}} + M_{2(q-1)} = \beta_{n_{2q-1}} + \alpha_1 - a \cdot 2M_{2(q-2)}N_{2q-3} - b \cdot 2M_{2(q-2)}N_{2q-3}$ when $a + b = N_{2q-2}$, $a, b = 1, 2, \ldots, N_{2q-2} - 1$. Clearly, $a \cdot 2M_{2(q-2)}N_{2q-3}d \in \mathbb{S}_{2(q-1)}$, $b \cdot 2M_{2(q-2)}N_{2q-3}d \in \mathbb{S}_{2(q-1)}$. Therefore, $\zeta_{\alpha_{n_{2q-1}}}$ and $\zeta_{\beta_{n_{2q}}}$ can be replaced by

$$\begin{aligned} \zeta_{\alpha_{n_{2q-1}}} &= \alpha_{n_{2q-1}} + M_{2(q-1)} , \\ \zeta_{\beta_{n_{2q}}} &= \beta_{n_{2q}} + M_{2(q-1)} , \end{aligned} \tag{81}$$

and then the sets of co-array lags in (78) remain the same as those in (56). As a result, the sensor positions of the extra two sub-arrays in (71) can be derived.

References

[1] H. Krim and M. Viberg, "Two decades of array signal processing research: the parametric approach," *IEEE Signal Process. Mag.*, vol. 13, no. 4, pp. 67–94, Jul. 1996.

[2] L. C. Godara, "Application of antenna arrays to mobile communications, part ii: Beam-forming and direction-of-arrival estimation," *Proceedings of the IEEE*, vol. 85, no. 8, pp. 1195–1245, August 1997.

[3] H. L. Van Trees, *Optimum Array Processing, Part IV of Detection, Estimation, and Modulation Theory*. New York: Wiley, 2002.

[4] T. E. Tuncer and B. Friedlander, *Classical and modern direction-of-arrival estimation*. New York: Academic Press, 2009.

[5] R. O. Schmidt, "Multiple emitter location and signal parameter estimation," *IEEE Trans. Antennas Propag.*, vol. 34, no. 3, pp. 276–280, Mar. 1986.

[6] R. Roy and T. Kailath, "ESPRIT-estimation of signal parameters via rotational invariance techniques," *IEEE Trans. Acoust., Speech, Signal Process.*, vol. 37, no. 7, pp. 984–995, Jul. 1989.

[7] D. Malioutov, M. Çetin, and A. S. Willsky, "A sparse signal reconstruction perspective for source localization with sensor arrays," *IEEE Trans. Signal Process.*, vol. 53, no. 8, pp. 3010–3022, Aug. 2005.

[8] Q. Shen, W. Liu, W. Cui, and S. Wu, "Underdetermined DOA estimation under the compressive sensing framework: A review," *IEEE Access*, vol. 4, pp. 8865–8878, 2016.

[9] A. Moffet, "Minimum-redundancy linear arrays," *IEEE Trans. Antennas Propag.*, vol. 16, no. 2, pp. 172–175, Mar. 1968.

[10] R. T. Hoctor and S. A. Kassam, "The unifying role of the coarray in aperture synthesis for coherent and incoherent imaging," *Proc. IEEE*, vol. 78, no. 4, pp. 735–752, Apr. 1990.

[11] M. B. Hawes and W. Liu, "Sparse array design for wideband beamforming with reduced complexity in tapped delay-lines," *IEEE Trans. Audio, Speech and Language Processing*, vol. 22, pp. 1236–1247, August 2014.

[12] P. Pal and P. P. Vaidyanathan, "Nested arrays: a novel approach to array processing with enhanced degrees of freedom," *IEEE Trans. Signal Process.*, vol. 58, no. 8, pp. 4167–4181, Aug. 2010.

[13] P. P. Vaidyanathan and P. Pal, "Sparse sensing with co-prime samplers and arrays," *IEEE Trans. Signal Process.*, vol. 59, no. 2, pp. 573–586, Feb. 2011.

[14] P. Pal and P. P. Vaidyanathan, "Coprime sampling and the MUSIC algorithm," in *Proc. IEEE Digital Signal Processing Workshop and IEEE Signal Processing Education Workshop (DSP/SPE)*, Sedona, AZ, Jan. 2011, pp. 289–294.

[15] S. Qin, Y. D. Zhang, and M. G. Amin, "Generalized coprime array configurations for direction-of-arrival estimation," *IEEE Transactions on Signal Processing*, vol. 63, no. 6, pp. 1377–1390, March 2015.

[16] C.-L. Liu and P. Vaidyanathan, "Super nested arrays: Linear sparse arrays with reduced mutual coupling-part i: Fundamentals," *IEEE Trans. Signal Process.*, vol. 64, no. 15, pp. 3997–4012, Aug. 2016.

[17] C.-L. Liu and P. P. Vaidyanathan, "Super nested arrays: Linear sparse arrays with reduced mutual coupling-part ii: High-order extensions," *IEEE Trans. Signal Process.*, vol. 64, no. 16, pp. 4203–4217, Aug. 2016.

[18] J. Liu, Y. Zhang, Y. Lu, S. Ren, and S. Cao, "Augmented nested arrays with enhanced DOF and reduced mutual coupling," *IEEE Trans. Signal Process.*, vol. 65, no. 21, pp. 5549–5563, Nov. 2017.

[19] A. Raza, W. Liu, and Q. Shen, "Thinned coprime arrays for DOA estimation," in *Proc. European Signal Processing Conference (EUSIPCO)*, Kos, Greece, Aug. 2017, pp. 395–399.

[20] A. Raza, W. Liu, and Q. Shen, "Thinned coprime array for second-order difference co-array generation with reduced mutual coupling," *IEEE Trans. Signal Process.*, vol. 67, no. 8, pp. 2052–2065, 2019.

[21] Y. D. Zhang, M. G. Amin, F. Ahmad, and B. Himed, "DOA estimation using a sparse uniform linear array with two CW signals of co-prime frequencies," in *Proc. IEEE International Workshop on Computational Advances in Multi-Sensor Adaptive Processing*, Saint Martin, Dec. 2013, pp. 404–407.

[22] Q. Shen, W. Liu, W. Cui, S. Wu, Y. D. Zhang, and M. G. Amin, "Wideband DOA estimation for uniform linear arrays based on the co-array concept," in *Proc. European Signal Processing Conference (EUSIPCO)*, Nice, France, Sep. 2015, pp. 2885–2889.

[23] E. BouDaher, Y. Jia, F. Ahmad, and M. G. Amin, "Multi-frequency co-prime arrays for high-resolution direction-of-arrival estimation," *IEEE Trans. Signal Process.*, vol. 63, no. 14, pp. 3797–3808, Jul. 2015.

[24] S. Qin, Y. D. Zhang, M. G. Amin, and B. Himed, "DOA estimation exploiting a uniform linear array with multiple co-prime frequencies," *Signal Processing*, vol. 130, pp. 37–46, Jan. 2017.

[25] K. Han and A. Nehorai, "Improved source number detection and direction estimation with nested arrays and ulas using jackknifing," *IEEE Trans. Signal Process.*, vol. 61, no. 23, pp. 6118–6128, Dec. 2013.

[26] K. Han and A. Nehorai, "Nested array processing for distributed sources," *IEEE Signal Process. Lett.*, vol. 21, no. 9, pp. 1111–1114, Sep. 2014.

[27] Y. D. Zhang, M. G. Amin, and B. Himed, "Sparsity-based DOA estimation using co-prime arrays," in *Proc. IEEE International Conference on Acoustics, Speech and Signal Processing (ICASSP)*, Vancouver, Canada, May 2013, pp. 3967–3971.

[28] Q. Shen, W. Liu, W. Cui, S. Wu, Y. D. Zhang, and M. G. Amin, "Low-complexity direction-of-arrival estimation based on wideband co-prime arrays," *IEEE/ACM Trans. Audio, Speech, Language Process.*, vol. 23, no. 9, pp. 1445–1456, Sep. 2015.

[29] Q. Shen, W. Cui, W. Liu, S. Wu, Y. D. Zhang, and M. G. Amin, "Under-determined wideband DOA estimation of off-grid sources employing the difference co-array concept," *Signal Processing*, vol. 130, pp. 299–304, 2017.

[30] C.-L. Liu and P. Vaidyanathan, "Cramér–rao bounds for coprime and other sparse arrays, which find more sources than sensors," *Digital Signal Processing*, vol. 61, pp. 43–61, 2016.

[31] A. Koochakzadeh and P. Pal, "Cramér–rao bounds for underdetermined source localization," *IEEE Signal Process. Lett.*, vol. 23, no. 7, pp. 919–923, 2016.

[32] M. Wang and A. Nehorai, "Coarrays, MUSIC, and the cramér–rao bound," *IEEE Trans. Signal Process.*, vol. 65, no. 4, pp. 933–946, Feb. 2017.

[33] J.-F. Cardoso and E. Moulines, "Asymptotic performance analysis of direction-finding algorithms based on fourth-order cumulants," *IEEE Trans. Signal Process.*, vol. 43, no. 1, pp. 214–224, Jan. 1995.

[34] M. C. Doğan and J. M. Mendel, "Applications of cumulants to array processing. i. aperture extension and array calibration," *IEEE Trans. Signal Process.*, vol. 43, no. 5, pp. 1200–1216, May 1995.

[35] P. Chevalier and A. Férréol, "On the virtual array concept for the fourth-order direction finding problem," *IEEE Trans. Signal Process.*, vol. 47, no. 9, pp. 2592–2595, Sep. 1999.

[36] P. Chevalier, L. Albera, A. Férréol, and P. Comon, "On the virtual array concept for higher order array processing," *IEEE Trans. Signal Process.*, vol. 53, no. 4, pp. 1254–1271, Apr. 2005.

[37] P. Chevalier, A. Férréol, and L. Albera, "High-resolution direction finding from higher order statistics: The $2q$-MUSIC algorithm," *IEEE Trans. Signal Process.*, vol. 54, no. 8, pp. 2986–2997, Aug. 2006.

[38] G. Birot, L. Albera, and P. Chevalier, "Sequential high-resolution direction finding from higher order statistics," *IEEE Trans. Signal Process.*, vol. 58, no. 8, pp. 4144–4155, Aug. 2010.

[39] P. Pal and P. Vaidyanathan, "Multiple level nested array: An efficient geometry for $2q$th order cumulant based array processing," *IEEE Trans. Signal Process.*, vol. 60, no. 3, pp. 1253–1269, Mar. 2012.

[40] Q. Shen, W. Liu, W. Cui, S. Wu, Y. D. Zhang, and M. G. Amin, "Group sparsity based wideband DOA estimation for co-prime arrays," in *Proc. IEEE China Summit and International Conference on Signal and Information Processing (ChinaSIP)*, Xi'an, China, Jul. 2014, pp. 252–256.

[41] Q. Shen, W. Liu, W. Cui, S. Wu, Y. D. Zhang, and M. G. Amin, "Focused compressive sensing for underdetermined wideband DOA estimation exploiting high-order difference coarrays," *IEEE Signal Process. Lett.*, vol. 24, no. 1, pp. 86–90, Jan. 2017.

[42] Q. Shen, W. Liu, W. Cui, and S. Wu, "Extension of nested arrays with the fourth-order difference co-array enhancement," in *Proc. IEEE International Conference on Acoustics, Speech and Signal Processing (ICASSP)*, Shanghai, China, Mar. 2016, pp. 2991–2995.

[43] Q. Shen, W. Liu, W. Cui, and S. Wu, "Extension of co-prime arrays based on the fourth-order difference co-array concept," *IEEE Signal Process. Lett.*, vol. 23, no. 5, pp. 615–619, May 2016.

[44] J. Cai, W. Liu, R. Zong, and Q. Shen, "An expanding and shift scheme for constructing fourth-order difference coarrays," *IEEE Signal Process. Lett.*, vol. 24, no. 4, pp. 480–484, Apr. 2017.

[45] A. Ahmed, Y. D. Zhang, and B. Himed, "Effective nested array design for fourth-order cumulant-based doa estimation," in *IEEE Radar Conference (RadarConf)*, 2017, pp. 0998–1002.

[46] T. H. Al Mahmud, Z. Ye, K. Shabir, R. Zheng, and M. S. Islam, "Off-grid DOA estimation aiding virtual extension of coprime arrays exploiting fourth order difference co-array with interpolation," *IEEE Access*, vol. 6, pp. 46 097–46 109, 2018.

[47] P. Gupta and M. Agrawal, "DOA estimation of non circular signals using fourth order cumulant in underdetermined cases," in *IEEE Workshop on Signal Processing Systems (SiPS)*, 2018.

[48] J. M. Mendel, "Tutorial on higher-order statistics (spectra) in signal processing and system theory: theoretical results and some applications," *Proc. IEEE*, vol. 79, no. 3, pp. 278–305, 1991.

[49] C.-L. Liu and P. P. Vaidyanathan, "Remarks on the spatial smoothing step in coarray MUSIC," *IEEE Signal Process. Lett.*, vol. 22, no. 9, pp. 1438–1442, Sep. 2015.

Qing Shen received his B.S. degree in 2009 and Ph.D. degree in 2016, both from Beijing Institute of Technology, Beijing, China. From 2013 to 2015, He was a visiting researcher in the Department of Electronic and Electrical Engineering, University of Sheffield, Sheffield, UK. He received two Excellent Ph.D. Thesis Awards from both the Chinese Institute of Electronics and Beijing Institute of Technology in 2016. He also received the First-Class Prize of the Science and Technology (Technological Invention) Award from Chinese Institute of Electronics in 2018, and the Second-Class Prize of the Ministerial Level Science and Technology Progress Award in 2014. His research interests include radar and array signal processing.

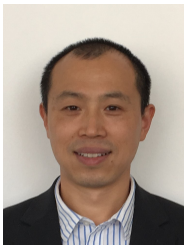

Wei Liu (S'01-M'04-SM'10) received his BSc and LLB. degrees from Peking University, China, in 1996 and 1997, respectively, MPhil from the University of Hong Kong in 2001, and PhD from the School of Electronics and Computer Science, University of Southampton, UK, in 2003. He then worked as a postdoc first at Southampton and later at the Department of Electrical and Electronic Engineering, Imperial College London. Since September 2005, he has been with the Department of Electronic and Electrical Engineering, University of Sheffield, UK, first as a Lecturer and then a Senior Lecturer. He has published more than 270 journal and conference papers, five book chapters, and two research monographs titled "Wideband Beamforming: Concepts and Techniques" (John Wiley, March 2010) and "Low-Cost Smart Antennas" (by Wiley-IEEE, March 2019), respectively. His research interests cover a wide range of topics in signal processing, with a focus on sensor array signal processing (beamforming and source separation/extraction, direction of arrival estimation, target tracking and localisation, etc.), and its various applications, such as robotics and autonomous systems, human computer interface, radar, sonar, satellite navigation, and wireless communications.

He is a member of the Digital Signal Processing Technical Committee of the IEEE Circuits and Systems Society and the Sensor Array and Multichannel Signal Processing Technical Committee of the IEEE Signal Processing Society (Vice-Chair from Jan 2019). He was an Associate Editor for IEEE Trans. on Signal Processing (March 2015-March 2019) and is currently an Associate Editor for IEEE Access, and an editorial board member ofthe Journal Frontiers of Information Technology and Electronic Engineering.

Wei Cui received the B.S. degree in physics and Ph.D. degree in Electronics Engineering from Beijing Institute of Technology, Beijing, China, in 1998 and 2003, respectively. From March 2003 to March 2005, he worked as a Post-Doctor in the School of Electronic and Information Engineering, Beijing Jiaotong University. Since then, he has been with the Beijing Institute of Technology, where he is currently a Professor with the School of Information and Electronics. His research interests include adaptive signal processing, array signal processing, sparse signal processing, and their various applications such as Radar, aerospace telemetry tracking and command. He has published more than 100 papers, holds 52 patents, and received the Ministerial Level Technology Advancement Award twice.

Siliang Wu received his Ph.D. degree in Electrical Engineering from Harbin Institute of Technology in 1995. He then worked as a post-doctor, and is now a professor in Beijing Institute of Technology. His current research interests include statistical signal processing, sensor array and multichannel signal processing, adaptive signal processing and their applications in radar, aerospace TT&C and satellite navigation. He has authored and co-authored more than 300 journal papers and holds 72 patents. He received the first-class prize of the National Award for Technological Invention, and the Ho Leung Ho Lee Foundation Prize in 2014. He is also the recipient of the State Council Special Allowance, the National Model Teacher, the National May 1 Labor Medal, and the National Outstanding Scientific and Technological Personnel.

Piya Pal (S'08-M'13) received her B.S. degree in electronics and electrical communication engineering from the Indian Institute of Technology, Kharagpur, and her Ph.D. degree in electrical engineering from the California Institute of Technology (Caltech), Pasadena, in 2007 and 2013, respectively. She is currently an assistant professor of electrical and computer engineering at the University of California, San Diego. Her research interests include signal representation and sampling for high-dimensional inference, super-resolution imaging, convex and non-convex optimization, and statistical learning. Her Ph.D thesis won the 2014 Charles and Ellen Wilts Prize for Outstanding Doctoral Thesis in Electrical Engineering at Caltech. Her research has been recognized by the 2016 NSF CAREER Award, the 2019 Office of Naval Research Young Investigator Program (ONR YIP) Award, and a 2018 Qualcomm Fellow Mentor Advisor Award. She and her student have received several best paper awards at conference, including the Best Student Paper Award at the IEEE International Conference on Acoustics, Speech, and Signal Processing (ICASSP) 2017. She is an elected member of the IEEE SAM and SPTM Technical Committees.